USE OF ABANDONED MINE DRAINAGE SOLIDS FOR THE CONTROL OF MERCURY EMISSIONS FROM COAL-FIRED POWER PLANTS

by

Wei Sun

B.S., Wuhan University of Technology, 2002

M.S., Shanghai Jiaotong University, 2006

Submitted to the Graduate Faculty of

Swanson School of Engineering in partial fulfillment

of the requirements for the degree of

Master of Science

University of Pittsburgh

2009

UNIVERSITY OF PITTSBURGH

SWANSON SCHOOL OF ENGINEERING

This thesis was presented

by

Wei Sun

It was defended on

April 2nd, 2009

and approved by

Radisav D. Vidic, Professor, Department of Civil and Environmental Engineering

Leonard W. Casson, Associate Professor, Department of Civil and Environmental Engineering

Jason D. Monnell, Research Assistant Professor, Department of Civil and Environmental Engineering

Thesis Advisor: Radisav D. Vidic, Professor, Department of Civil and Environmental Engineering

USE OF ABANDONED MINE DRAINAGE SOLIDS FOR THE CONTROL OF MERCURY EMISSIONS FROM COAL-FIRED POWER PLANTS

Wei Sun, M.S.

University of Pittsburgh, 2009

Abandoned mine drainage (AMD) solids were evaluated for their ability to capture mercury from the flue gas of coal fired power plants. A fixed bed system was used to test Hg adsorption and oxidation by this material in a typical simulated flue gas. Fixed-bed tests showed that abandoned mine drainage from three mines displayed considerable capability for absorbing and oxidizing Hg^0. Among all the flue gas components, HCl showed the greatest impact on Hg capture in the fixed-bed test, while O_2 was shown to be not as important. A decrease in mercury capture and oxidation was observed when SO_2 and NO_2 were added to the flue gas. The addition of SO_2 and NO prohibited mercury uptake but showed no impact on Hg oxidation.

An entrained flow system was utilized to test mercury removal efficiency when abandoned mine drainage solids were injected into the flue gas. Four different AMD solids were tested using both eastern coal and PRB coal flue gas. Results showed that one AMD sample achieved about 80% Hg removal at the solids injection rate of 0.39 g/m^3 injection rate. Mercury removal efficiency with other AMD samples under the identical conditions ranged from 25%~50%. Thus, this material shows great potential as a novel sorbent on Hg emission control technology. Moreover, Hg removal efficiency was found to be positively related to the iron content of AMD solids. Therefore, AMD solids with high iron content would be more desirable as mercury removal sorbent.

The foam index test was also performed using this material to study the possible effect of AMD solids on the application of fly ash in concrete making, which is the main disadvantage of activated carbon injection technology. The test results indicated that all AMD samples used in this study would not have any adverse effect on the fly ash with regards to its application for concrete making.

Keyword: Abandoned mine drainage, Flue gas, Mercury adsorption, Mercury oxidation, Mercury removal, Injection.

TABLE OF CONTENTS

LIST OF TABLES

LIST OF FIGURES

ACKNOWLEDGEMENTS

First of all, I would like to thank my academic advisor, Dr. Radisav D. Vidic. I am highly grateful for his advice, not only on my research work but also more importantly, on my way of thinking. His superior professional standards on research have always driven me to strive for perfection. His insight into different research areas and enthusiastic research attitude also impressed me so much.

I will give my great thanks to Dr. Jason D. Monnell for his unreserved help for me to achieve my research and academic goals. This invaluable help undoubtedly makes my life and research work here much easier.

A great thank also goes to Dr. Leonard W. Casson. What he taught to me is not only the priceless knowledge in courses but also to always keep the invaluable engineering concepts in mind.

I am thankful to Dr. Robert S. Hedin for providing the AMD sludge samples and the elemental analysis.

This study was supported by the National Energy Technology Laboratory (NETL), USDOE. I would like to thank all my colleagues and friends, Xihua Chen, Ravi Bhardwaj, Huixing Li, Sean Shih, Heng Li, Kent Pu and Hui Liu for their support and help with daily work and study. Finally, I would send my greatest appreciation to my wife, sister and parents in China, who never hesitate to show their love and support to me.

1.0 INTRODUCTION

Coal fired utility boilers are the largest mercury emission sources caused by human activities. In US, they are responsible for one-third of the Hg emission from the combustion point sources.[1] The mercury species in flue gas vary based on the type of coal combustion conditions used in the plants and mercury removed by existing air pollution control device (APCD) in power plants is highly influenced by mercury speciation.[1]

Among different mercury emission control technologies, activated carbon injection (ACI) technology has shown the most promise as a near-term technology. It has been widely studied and applied as an effective means of mercury capture from flue gas and. This technology involves injection of powdered activated carbon (PAC) upstream of a particulate control device (e.g., electrostatic precipitator or fabric filter). Mercury in the combustion flue gas is then adsorbed on PAC and PAC is subsequently captured along with the fly ash in the particulate control device. One of the key disadvantages of ACI technology comes from the fact that activated carbon usage could increase the carbon content in fly ash, which has negative impact on fly ash sale for concrete application.

Abandoned mine drainage (AMD) refers to outflow of contaminated water from abandoned coal mines or metal mines. AMD can have severe adverse impacts on the aquatic environment and should be treated prior to discharge. The solids created by AMD treatment commonly contain significant fraction of iron oxide/hydroxide and are collected and disposed in

secured landfills or injected back into the abandoned mine. AMD solids do not have many known beneficial reuse applications except as pigments in dye manufacturing.[2]

Previous studies revealed that iron oxide is be capable of adsorbing and oxidizing Hg in simulated flue gas.[3] Literature review also shows that iron oxide present in fly ash has the capability to oxidize/capture elemental mercury in flue gas.[4] Accordingly, it may be possible to utilize iron oxide recovered from sludge in AMD treatment as a novel sorbent to remove Hg from flue gas. Therefore, the purpose of this study was to evaluate the capability of AMD solids for Hg removal in simulated flue gas and investigate the feasibility of using this novel sorbent material for air pollution control in thermoelectric power plants. This overall objective can be divided into following specific objectives:

1) Evaluate the Hg adsorption and oxidation capability of AMD solids in a fixed bed system using both eastern coal and PRB coal flue gas.

2) Study the impact of flue gas compositions on mercury uptake and oxidation with AMD solids.

3) Evaluate the performance of selected AMD solids under more realistic process condition (i.e., in the entrained flow system) for mercury removal in both eastern coal and PRB coal flue gas.

4) Investigate the impact of AMD solids as mercury removal sorbent on fly ash for concrete preparation.

2.0 LITERATURE REVIEW

2.1 MERCURY EMISSION FROM COAL-FIRED POWER PLANTS

Mercury exists in trace amounts in coal, waste and other material. When these materials burn, mercury is released into the air. As shown in Figure 1, coal-fired power plants contributed about 33% of the total US anthropogenic mercury emissions in 1995. When mercury is deposited in water or land, it can be changed by bacteria from metal form into methyl mercury (MeHg), which can bioaccumulate in the food chain. Since mercury has great toxic effects on environment and human health, it is considered as one of the most important trace elements emitted from coal-fired power plants. In the US, the consumption of contaminated fish is the primary source of mercury exposure. Forty one states have issued advisories to limit consumptions of predatory fish species.[5] New research studies have shown that Hg in atmosphere exists as either elemental (Hg^0), oxidized mercury (Hg^{2+}), or particulate-bound mercury (Hg_p). Elemental mercury has an atmospheric life time of between 12 and 18 months, which causes its transport around the globe before deposition. The atmospheric life time of oxidized mercury is between 5-14 days and it tends to be deposited on land locally to the source. Particulate-bound Hg also shows similar behavior. [6, 7]

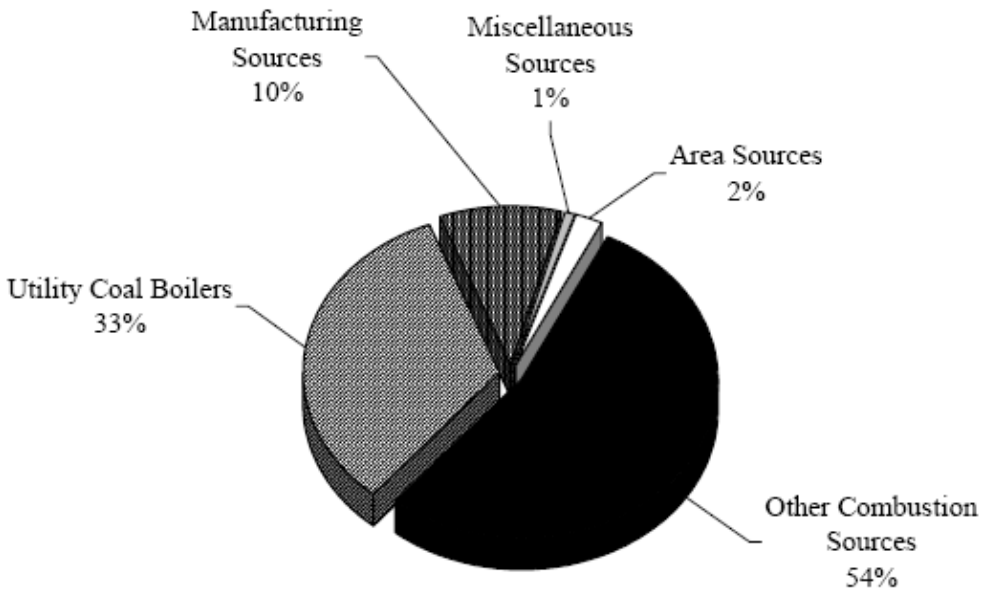

Figure 2.1. Source contributions to 1995 Total US Anthropogenic mercury emission [8]

In 1999, EPA issued a three-part Information Collection Request (ICR) to obtain the data on the amount of mercury in US coals and mercury emissions from coal-fired power plants.[9] From the mercury emissions estimates reported by EPRI and EPA based on ICR data, approximately 75 tons of mercury entered coal-fired utility boilers during 1999 and about 45 tons were discharged into the atmosphere. On average, about 40% of the mercury was retained in the residues of combustion such as bottom ash, fly ash and scrubber sludge and this percentage number varied from under 10% to 90% depending on coal type and plant design.[10, 11]

Particulate-bound Hg in flue gas from coal-fired power plants is easily removed using control equipment such as ESP or fabric filter. Wet flue gas desulfurization scrubber can remove high levels of Hg^{2+} since it is highly soluble in water. However, Hg^{0} is difficult to remove because it is relatively insoluble in water and highly volatile. Table 2.1 presents the mercury removals from flue gas for various control technologies.

Table 2.1 Control technology categories and estimated mercury removal ranked by tons of mercury entering plants[11]

Control category	Tons of mercury entering	Number of U.S. power plants	Number of part III test sites	Estimated mercury removals, %			Mercury emission calculation, EPRI ICR, tons
				ICR EPRI 2000	ICR	EPA, 1996	
ESP cold	39.4	674	18	27	39	32	28.8
ESP cold+ FGD wet	16.8	117	11	49	64	66	8.6
ESP hot	5.5	120	9	4	29		5.3
Fabric filter	2.9	58	9	58	56	44	1.2
Venturi Particulate scrubber	2.2	32	9	18			1.8
Spray dryer+ fabric filter	1.6	47	10	38		30	1
ESP hot + FGD wet	1.6	20	6	26	54		1.2
Fabric filter +FGD wet	1.5	14	2	88	81	78	0.2
Spray dryer + ESP cold	0.3	5	3	18			0.2
FBC+ fabric filter	3.4	39	5	86			0.5
IGCC	0.07	2	2	4			0.1
FBC +ESP cold	0.02	1	1				
Totals	75.3	1128	84				48.8

The ICR data provides the available information to study the effectiveness of existing technologies and their capability to reduce mercury emission. In the ICR tests, close to 100% of mercury burning in coal was emitted ahead of a particulate control device.[12] Mercury speciation was predominantly affected by coal chlorine content and the temperature in Figure 2.2.[12]

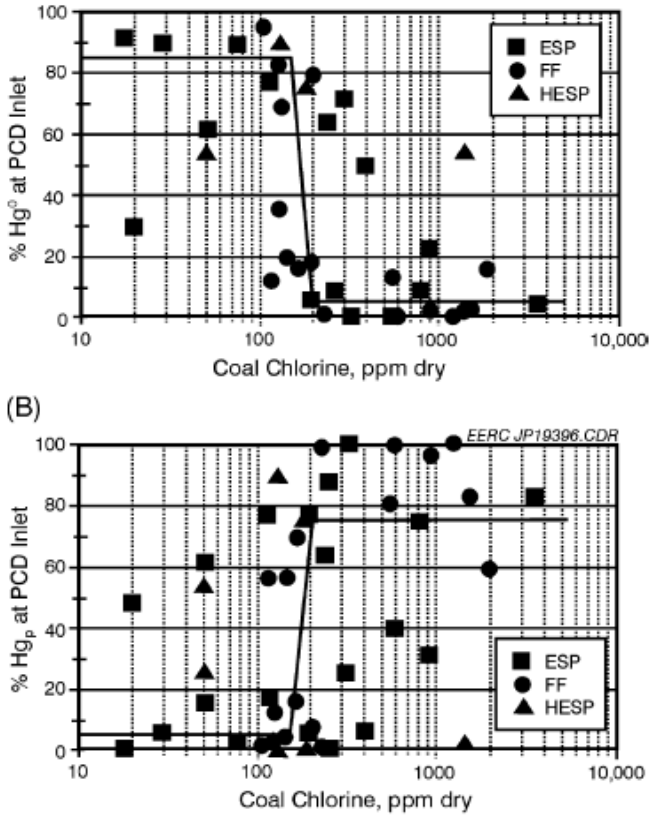

Figure 2. 2. Percentage of mercury as (A) gas phase elemental and (B) particulate bound at the inlet to particulate control devices (PCDs) based on ICR data[12]

The percentage of Hg leaving the boiler in elemental form decreased sharply from over 85% to about 10% for coal chlorine contents greater than 150~200pm.

Particulate control devices (PCD) can also influence mercury emission. 75% of coal-fired power plants have only particulate controls, and 80% of these facilities are cold-side or hot-side ESP or a fabric filter (FF). As shown in Table 2, average Hg removal efficiency for these categories are 27%, 4% and 58%, respectively.[13] Fig 2.3 shows the removal of gaseous mercury across the PCD as a function of coal chlorine content based on ICR data.

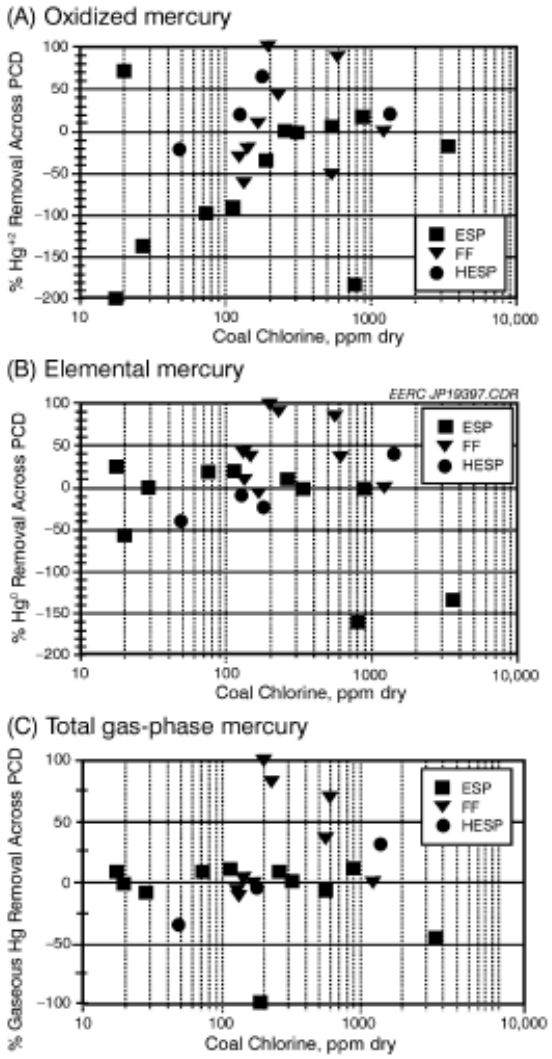

Figure 2.3. Removal of gaseous mercury across PCD as a function of coal chlorine content based on ICR data[12]

151 power plants in U.S. have installed wet flue gas desulfurization (WFGD) systems to control the SO_2 emission, which represents about 25% of all coal-fired utility generating capacity. ICR tests on WFGD units followed a cold side-ESP, a hot side-ESP or a FF. The result showed that typically about 90% of the oxidized gaseous mercury entering flue gas system was removed. However, elemental Hg was not eliminated and appeared to increase slightly in some tests. The possible reason for this was that ionic mercury was chemically reduced by sulfite in the scrubber

solution and then reemitted as elemental Hg.[12] The influence of the coal chlorine content on mercury removal across scrubbers and particulate controls devices is shown in Figure 2.4.

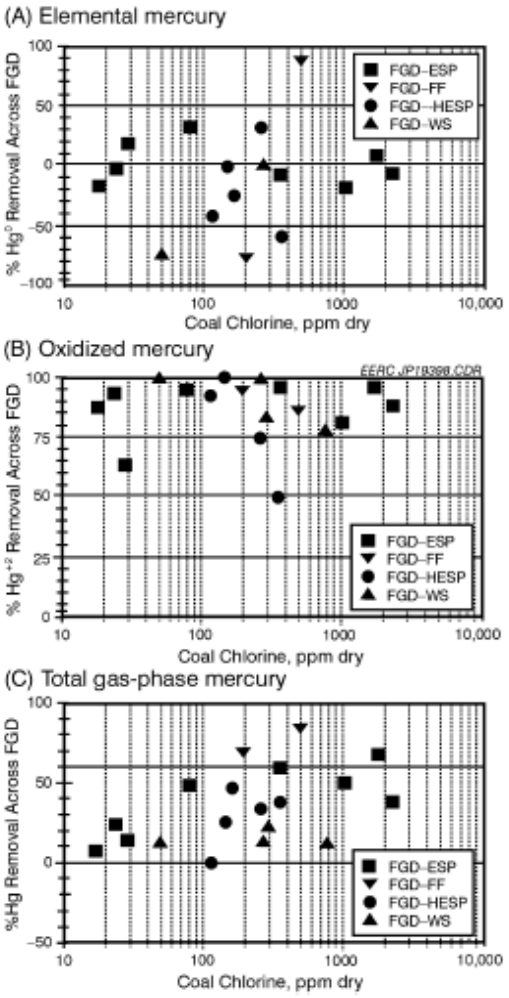

Figure 2.4. Removal of gaseous mercury across FGD as a function of coal chlorine content based on ICR data[12]

As Figure 4 shows, removal of mercury across FGD alone was approximately doubled from 30% to 60% following a CS-ESP with an increase of chlorine content in coal from 50 to 1000 ppm chlorine. And it also increased from about 20% to 50% when following a hot side-ESP with an increase of chlorine content in coal from 200 and 1000 ppm chlorine in coal.[13]

FGD following a FF achieved the highest combined removal of about 88%, where 77% removal of the mercury entering the scrubber contributed by FF was in an oxidized form. FGD following a hot side- ESP achieved only 26% mercury removal on average.[14]

Spray dryer absorber uses alkaline (typically lime) slurry to absorb SO_2. The dry sorbent and fly ash particulates are captured in FF or ESP. Spray dryer absorber can also remove about 90% of the oxidized gaseous mercury. The systems equipped with FF can eliminate a significant fraction of elemental mercury when more than 200ppm chlorine content existed in the coal.[12] Total mercury removal in combined spray dryer and FF varied from 0% to 99% at 10 ICR test Sites with an average removal of 38% removal. The total average mercury removal across spray dryer following an ESP of three ICR test Sites was 18%.

Investigators in Europe have reported that Hg^0 was completely oxidized to $HgCl_2$ on the surface of SCR catalyst in the presence of HCl in laboratory tests. In full-scale power plants elemental mercury decreased slightly from 40%-60% to 2%-12%.[1] The effect of the SCR catalyst was considered to be affected by reducing gases and fly ash. Energy and Environmental Research Center (EERC) reported that the fraction of particulate-bound mercury across the SCR increased substantially when burning two high-chlorine eastern bituminous coals in pilot-scale tests. However, there is no effect of SCR on Hg species change when burning a low-chlorine Powder River Basin (PRB) subbituminous coal. Changes in Hg species are affected by coal burned, operating temperature and ammonia concentrations in the flue gas.[15]

2.2 ACTIVATED CARBON INJECTION (ACI) TECHNOLOGY

In ACI technology, powdered activated carbon (PAC) sorbent is injected into the flue gas at the location in the duct upstream of the particulate matter (PM) control devices (usually an electrostatic precipitator or a fabric filter). The PAC sorbents adsorbs mercury in the flue gas in the duct and is removed in the PM control device. Since gas-particle contact is enhanced in the filter cakes on the surface of the bags in a FF, higher mercury removal is observed with a fabric filter compared to an ESP.

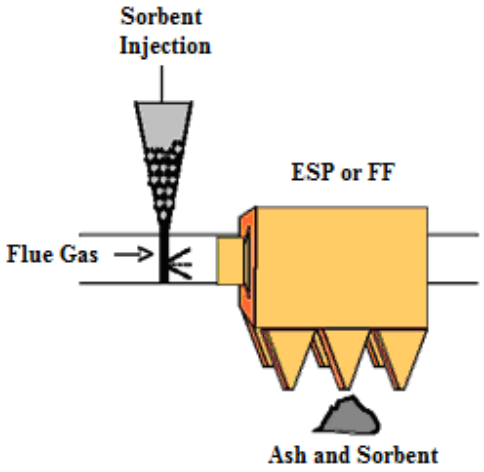

Figure 2.5. Schematic of Activated carbon injection for mercury control [16]

The physical and chemical characteristics of activated carbon determine its performance for mercury removal. Generally, the physical properties of interest are surface area, pore size distribution and particle size distribution. In general the capacity for Hg capture increases with increasing surface area and pore volume. The ability of Hg to enter the interior of a particle is related to the pore size distribution and the pores of the activated carbon sorbent should be large enough for Hg^0 and Hg^{2+} to access to the internal surface. When PAC particle

size decreases, the distance to the adsorption site on the internal surface area of the particle decreases and the adsorption rates increases.[16]

Many full scale tests have been performed to evaluate activated carbon injection for mercury control in coal-fired power plants. From 2001 to 2006 ADA-ES was working under a DOE NETL cooperative agreement to assess the costs of controlling mercury from coal-fired plants using PAC injection based on various levels of mercury control.[17] The test results showed that activated carbon was effective on both elemental and oxidized mercury species. In contrast to wet scrubbers, these tests showed that PAC was capable of treating flue gas from both bituminous and subbituminous coals. The type of particulate control equipment is the most important parameter influencing the performance of ACI. Only 2-4 lb/Macf of carbon injection rate could obtain 90% of Hg removal with a fabric filter, while in an ESP at least 10 lb/Macf was required to achieve about 70% removal. Tests with a PRB ash indicated that the presence of even small amounts of activated carbon in the ash would cause the material to be unacceptable for use in concrete production. In addition the COHPAC baghouse configuration was used to collect the ash upstream of the carbon injection so the ash still could be acceptable for sale.[17]

Energy & Environmental Research Center (EERC) reported the results of field testing result of activated carbon injection at TXU's Big Brown Station.[18] This test investigated the long-term feasibility of cost-effective mercury removal from Texas lignite-subbituminous blends at TXU's Big Brown Station using activated carbon injection with and without additives or enhancements. The results showed that activated carbon injection of about 4 lb/Macf can attain 80% of Hg removal.

Recent test results indicate that brominated activated carbons achieve higher mercury removal from flue gas at lower injection rate than original activated carbon. Sorbent

Technologies Corporation tested injection of brominated powdered activated carbon (B-PAC^{TM}) at seven different power plants. These plants have burning bituminous, subbituminous or lignite coals and equipped with cold-side ESP, hot-side ESP, spray dryers or fabric filters. Mercury removal in these tests varied between 70% and 98% for brominated activated carbon injection rate of 1 lb/MMacf to 2.5 lb/MMacf. With the same injection rate Norit Darco FGD PAC can only attain about 30% ~ 80% of Hg removal efficiency. [19]

PAC injection can have two types of negative impact on the potential use of fly ash in concrete. Fly ash samples with even low concentrations of carbon would be discolored. The darker color would make this material less marketable compared with other ash material without PAC injection. The second impact, which is more important, is that the fly ash with PAC could fail the foam index test. Foam index test is used to determine the amount of Air Entrainment Additives needed to meet freeze thaw requirements for concrete. This means that PAC injection would reduce revenues from ash sales for plant and increase the additional expenses to landfill this material.[1, 20, 21] Therefore, several studies were focused cost-effective non-carbon sorbent to control mercury emissions from coal-fired power plans. [22, 4,23,24]

Iron and its oxides were found to be able to catalyze Hg^0 oxidation.[1] Ferric oxide was tested for its ability to oxide elemental mercury in eastern coal flue gas at 140°*C* using the fixed bed reactor.[3] The test result showed that ferric oxide was able to adsorb and oxidize Hg^0 under these conditions. This test revealed that about 40% of mercury exiting the reactor after 300 minutes of continuous feed existed as oxidized mercury. Moreover, the capacity of ferric oxide on mercury uptake was 42.5 μg Hg/g. Dunham et.al.[25] observed that the extent of mercury oxidation in the presence of fly ash increased at 120 and 180°*C* when the magnetite (Fe_3O_4) content of the fly ash increased. Ghorishi et al. [26] exposed simulated flue gas comprised of HCl

to model fly ashes in a fixed bed system and found that 90% of Hg oxidation was achieved by the Fe_2O_3 containing ash at 150°*C*. When Fe_2O_3 was removed from the model fly ash, only 10% of Hg^0 was converted to Hg^{2+}. This result suggested that Fe_2O_3 in the ash catalyzed oxidation of Hg^0 to Hg^{2+}. Galbreath et al.[27] injected α- Fe_2O_3 and γ- Fe_2O_3 into the flue gas with fly ash. It was found that Hg speciation in the flue gas was not changed by injection of α- Fe_2O_3. γ- Fe_2O_3 injection increased the extent of Hg oxidation when being coated onto baghouse filters. Wu. et al.[28] developed a process for the Hg^0 removal using H_2S over iron oxides sorbents. In this study the sulfidation behavior and activity for COS formation were investigated during Hg^0 removal from coal derived fuel gas over iron oxides prepared by conventional impregnation.[28] Qiu et al.[29] studied the element mercury oxidation by α- Fe_2O_3 and γ- Fe_2O_3 nanoparticles. In this study α- Fe_2O_3 and γ- Fe_2O_3 nanoparticles were investigated for the heterogeneous interactions with elemental mercury in simulated flue gas. It was found that α- Fe_2O_3 and γ- Fe_2O_3 powders with ordinary size of around 150 μ m could not catalyze and oxidize elemental Hg, which conflicts with the finding ins other studies. [25, 26, 27] On the other hand, α- Fe_2O_3 and γ- Fe_2O_3 nanoparticles showed ability to oxidize Hg^0 with about 40% of oxidation efficiency. The increase of temperature will cause an obvious increase in mercury oxidation efficiency for both types of Fe_2O_3 nanoparticles,

2.3 ABANDONED MINE DRAINAGE SLUDGE

Abandoned mine drainage, or AMD, is water that is discharged from abandoned mine once they are filled with water.. Abandoned mine drainage contamination results when the

mineral pyrite (FeS_2) is exposed to air and water, resulting in the formation of sulfuric acid and iron hydroxide. The production process of abandoned mine drainage occurs deep underground or in spoils piles with the oxidation of the mineral pyrite, which is associated with coal and some shales. The chemistry of abandoned mine drainage can be described as following:

pyrite	water	dissolved oxygen		ferrous iron		sulfate		hydrogen ion	
$FeS_{2,s}$	+ H_2O	+ $7/2\ O_2$	=	Fe^{2+}	+	$2SO_4^{2-}$	+	$2\ H^+$	(1)

Fe^{2+} does not precipitate from solution unless pH is very high. If sufficient oxygen exists in the water, ferrous iron is oxidized to make ferric iron shown below. This reaction causes pH to increase.

ferrous iron	dissolved oxygen		hydrogen ion		ferric iron		water	
Fe^{2+}	+ $1/4O_2$	+	H^+	=	Fe^{3+}	+	$1/2H_2O$	(2)

If pH value is above approximately 3.5, the ferric iron will react with water to form a solid iron hydroxide precipitate according to:

ferric iron	water		ferric hydroxide		hydrogen ion	
Fe^{3+}	+ $3H_2O$	=	$Fe(OH)_{3,s}$	+	$3H^+$	(3)

Abandoned mine drainage can have severe impact on the environment, such as contaminating groundwater, raising water treatment costs and affecting the ordinary growth of terrestrial plants.[13] Many studies have evaluated to chemical reactions that create the acidity and

the precipitation of dissolved metals. Although improvements have been made in prediction and prevention, the problems of abandoned mine drainage still exist.

Abandoned mine drainage treatment generally includes two broad categories: active and passive treatment. Active treatment involves adding a neutralizing chemicals physically to the source of the abandoned mine drainage or directly to the stream which has been impacted.[30] The widely used chemicals are limestone, hydrated lime, soda ash, caustic soda and ammonia. In general, the active treatment systems consist of reaction tank, flash/flocc mixing tank, plate clarifier, a filter press and a settling pond. This technology can be very successful. However, it requires a long-term and continuous commitment to treatment. Weather, equipment failure and budget reductions can result in the failure in the treatment. [30]

Since the early 1990s, passive treatment system has been developed to treat AMD. Passive treatment of abandoned mine drainage consists of raising the pH to reduce metal loading through a constructed treatment or containment project, such as constructed wetlands, open limestone channels /Anoxic Limestone Drains and diversion wells. Compared with the active treatment, the initial costs of passive treatment technology is higher, but it is more uniform and utilizes processes which require no intensive labor and maintenance.[30]

A major challenge in AMD treatment is the management of large volumes of loose sludge generated through neutralization.[2, 31] Since AMD is produced in large amounts worldwide, it is difficult to assess the scale of the sludge volume generated from AMD treatment. [32] Generally AMD sludge is composed of a mixture of various metal hydroxides and/or oxides. The ultimate chemical composition depends on the AMD characteristics and treatment method.[33] For example, AMD sludge from lime treatment is typically high in Ca due to the presence of gypsum or unreacted lime (up to 40%). [34]

Commonly active AMD treatment involves with chemical addition (lime and coagulants) followed by aeration and retention in sedimentation ponds. The resulting sludge containing iron oxide/hydroxide is collected and disposed by landfilling or injection into the abandoned mine after the treatment.[35] A few studies have been conducted on the beneficial application of abandoned mine drainage sludge. Active treatment facilities have lower Fe concentration in AMD sludge since sludge is diluted by the chemicals addition. The color of the AMD sludge from active treatment facility exhibits considerable variations.[33] Abandoned mine drainage sludge was studied as an adsorbent for a cost-effective treatment approach to phosphorus removal from municipal secondary effluents.[36] Adsorption of orthophosphate onto AMD sludge particles followed the Freundlich isotherm model with an adsorption capacity ranging from 9.89 mg/g to 31.97 mg/g and more than 98% of phosphorus removal efficiency was achieved in treating municipal secondary effluent. Moreover, AMD sludge has been used as a raw material to produce pigment or coagulants.[32] The wetland facilities used to treat AMD concentrate Fe in the similar way in which nature concentrates Fe from weathered rock. It was found that the Fe concentration in sediments from wetland mine drainage treatment facility exists in the range of natural pigments. The AMD sludge from passive treatment wetlands was considered as a resources for pigment or other uses of ferric oxides. [37]

2.4 SUMMARY AND RESEARCH NEEDS

Literature review indicates that activated carbon injection technology can have adverse impacts on beneficial reuse of fly ash application due to fly ash discoloration by carbon and due to the fact that the fly ash containing PAC can fail the Foam Index Test. Previously studies found

that iron oxide was capable of absorbing and oxidizing Hg in flue gas. AMD sludge contains high concentration of iron oxide and can possibly serve as a new sorbent for Hg removal in Hg emission control technology. This novel material was evaluated for Hg removal in fixed-bed system and entrained flow reactor with simulated flue gas. In addition, the impact of this material on fly ash performance in concrete manufacturing was also investigated in this study.

3.0 MATERIAL AND METHODS

3.1 ABANDONED MINE DRAINAGE MATERIAL SAMPLES

Five samples of AMD solids named Site A, Site B, Site C, Site1, Site 2 and Site 3 were used in this research; these samples were collected from four different abandoned mine drainage treatment sites as described below.

Site A sample is recovered from a site of a large system of ponds and wetlands that passively treats a large AMD discharge. The system precipitates most of the iron contamination in ponds designed for sludge removal, while residual iron is removed in a constructed wetland and then recovered to produce pigment-quality iron oxide. All the design follows the patent, "Recovery of Iron Oxides from Polluted Coal Mine Drainage" (USPTO Patent No. 5,954,969). [35] The chemical composition of Site A sample is presented in Section 4.

Site B samples were obtained from a treatment plant in McMurray PA (Washington County). The plant pumps 3500 gpm of mine water (pH 6.5, Fe 40 mg/L) that is treated with aeration followed by lime addition and settling. The water is pumped into a basin where it is aggressively aerated to remove CO_2, which raises the pH to 7 and makes subsequent lime treatment more efficient. The basin collects iron sludge. The Site B sample was collected from the end of the aeration basin, before the addition of lime.

Site C samples were collected from an AMD seepage zone in Farmington Township, PA (Clarion County). The iron oxide was produced by a 55 gpm natural spring (pH 5.8, Fe 110 mg/L) that had polluted Little Coon Creek over the last 50 years. Iron oxide sludge is accumulated in a flat area between the spring and the stream. During the construction of a passive treatment system in 2007, the iron sludge was removed and processed (passive drying and screening). The samples were collected from this processed material.

Site 1 sample is produced from an AMD treating water from a mined-out, flooded, Pittsburgh seam mine. The raw water was rich in bicarbonate content and relatively low ferrous iron content. Unit operations at the treatment plant include: 1) preaeration using high speed mechanical aerators, 2) Addition of hydrated lime with more mechanical aeration and 3) gravity sedimentation in an open pond. After drying, Site 1 AMD solids will be composed primarily of calcium carbonate (a reaction product of the lime and the native bicarbonate present in the raw water) and iron oxyhydroxides. Site 1 sample and Site B sample were from the same site, but Site B sample was collected before lime addition.

Site 2 utilizes the High Density Sludge process in which the sludge is settled in a clarifier rather than an open pond. The majority of the settled sludge from the underflow of the clarifier is recycled through a high pH zone and returned to the process at the aeration basin. Recirculation of high pH sludge is supposed to impart a negative surface charge to the particles that will attract the dissolved ferrous iron to the particle surface. The objective is for iron oxidation to occur at the surface of an existing particle so that particle growth is achieved and new particle formation is avoided.

Site 3 treats water that is a combination of water from a mined-out, flooded Freeport seam mine water from overlying Pittsburgh seam deep mines and runoff/leachate from a refuse

disposal area (largely Freeport refuse). The raw water is highly mineralized (ferrous iron, acidity due to dissolved metals and sulfate are all high) and has a higher manganese content than the other waters. The unit operations for the treatment plant are the same as for Site B, but the water was treated to a higher pH (~9.0) to remove the manganese effectively. The sludge is highly expected to contain ferric oxyhydroxide, calcium sulfate and calcium carbonate as major components with a somewhat higher manganese and aluminum content than the other sites.

Site A, Site B, Site C, Site 1 and 2 are ground and sieved to the particle size below 37μm for the fixed bed and entrained flow experiments. Site 3 sample is used without sieving since particle size analysis of Site 3 sample after grinding shows that it is not necessary to sieve it.

3.2 EXPERIMENTAL SETUP AND PROCEDURE

3.2.1 Fixed bed system setup

The fixed bed system in this research consists of the following parts: 1) mercury generator, 2) simulated flue gas system, 3) fixed bed reactor, 4) mercury analyzer system. Figure 3.1 shows the schematic of the fixed bed system.

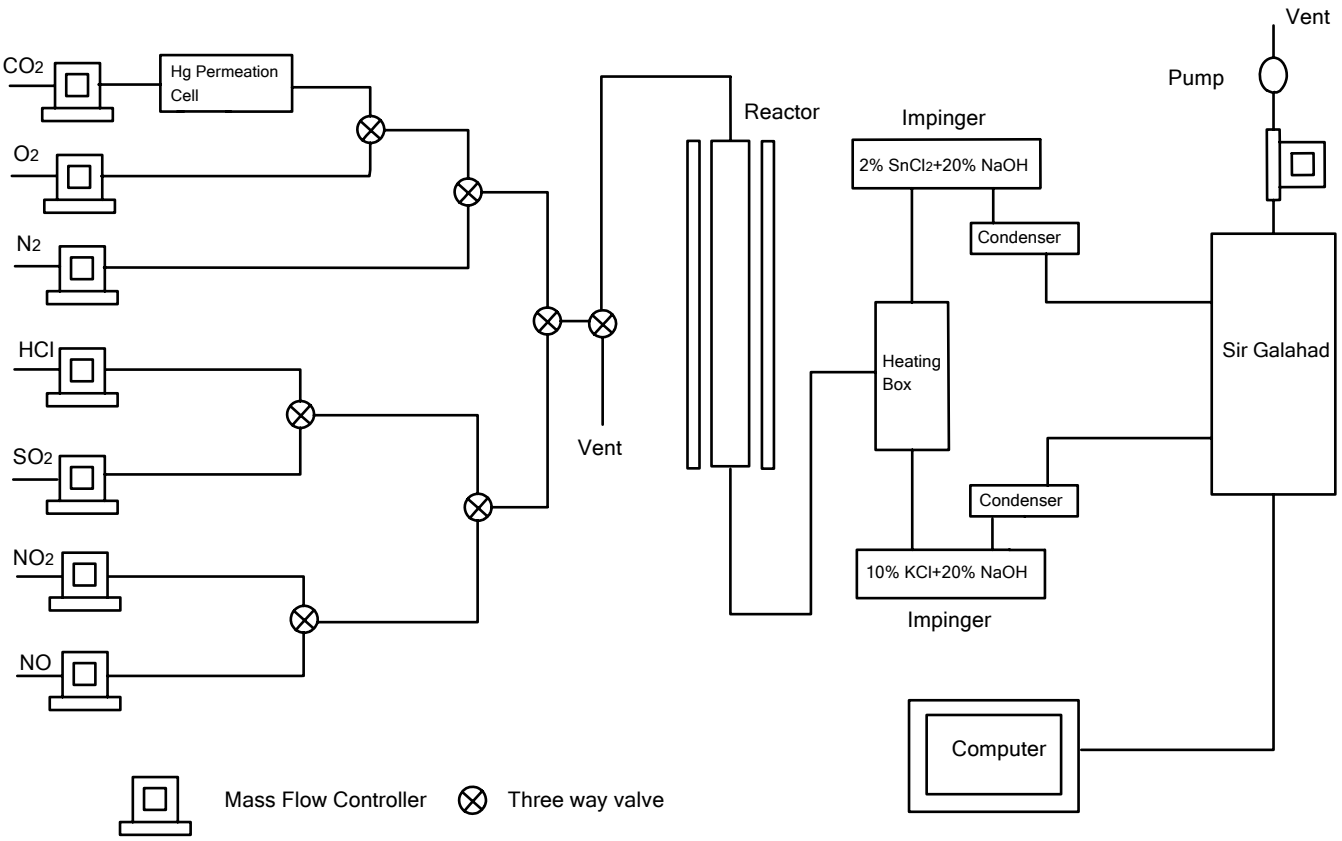

Figure 3.1. Schematic of fixed -bed set up

A simulated flue gas comprised of N_2, CO_2, O_2, HCl, NO, NO_2 and SO_2 was generated in this study. The compositions of flue gas from the power plants burning Eastern coal and Powder River Basin (PRB) coal were selected for this study. The compositions of those two flue gases were listed in Table 3.1.[20, 38]

Table 3. 1. Compositions of eastern coal flue gas and PRB flue gas

Gas Compositions	Conc. In Eastern coal flue gas	Conc. In PRB flue gas
CO_2	13.5%	13.5%
O_2	6%	6%
HCl	50 ppm	10ppm
NO	300 ppm	300 ppm
NO_2	20 ppm	20 ppm
SO_2	0.15%	300 ppm
N_2	Balance	Balance

The source of elemental mercury is a mercury permeation tube (VICI Metronics, Santa Clara, CA). This permeation tube was designed to produce elemental Hg vapor as function of temperature only. It was placed in a U-tube glass, which was heated by a temperature controlled oil bath. When carrier gas was introduced into the U-tube glass, the elemental Hg vapor produced by the permeation tube would be picked up and mix with other gases to produce the simulated flue gas. The temperature of oil bath can be adjusted to attain the desired Hg concentration in the study.[39]

In a fixed bed test, simulated flue gas with 1L/min flow rate was introduced into a quartz reactor (29cm long with 20 mm ID). This reactor was heated to a desired temperature by a tubular furnace (Lindberg Heavi-Duty, Watertown, WI) with a temperature controller. The effluent stream was sent to PSA Sir Galahad II System to analyze total and elemental mercury concentration.

Mercury analysis system in this research involved a wet condition system. This system was utilized not only to remove the acid gas and moisture but also to produce the appropriate sampling gas from the effluent flue gas for the Hg analyzer. In the gas conditioning system the effluent gas passes through a heating box, which prevents oxidized mercury from being absorbed on the tubing. The gas is then spilt into two streams in the heating box. One stream is directed to

the total side through 2% $SnCl_2$ + 20% NaOH solution that is used to reduce oxidized mercury to elemental form and remove acid gases. This stream is used to measure total mercury in the effluent from the reactor. The other stream is directed through 10% KCl +20% NaOH solution that is used to remove oxidized mercury and acid gases. This stream is used to measure elemental mercury in the effluent from the reactor. Both streams would pass through a chiller in order to condense the moisture in the gas before it entered the Hg analyzer. [39]

After the wet conditioning system the effluent gas is introduced into PSA 10.525 Sir Galahad II (P S Analytical Ltd, Orpington, Kent, England) to perform the Hg analysis. This Hg analyzer is based on the mechanism of atomic fluorescence measurement. A gold sand trap is used to adsorb any mercury directed into this trap during the sampling phase. After the sampling phase, argon was introduced to flush any residual gases from the sand trap to eliminate their possible interference with mercury analysis. The trap is then heated to about 500°C and the desorbed mercury is carried into a fluorescence detector by argon gas. A solenoid valve controlled by a timer was used to switch the gas flows to Sir Galahad from the elemental side or from the total side one after another. The flow rate of the sample gas was maintained as 200ml/min during a 60s sampling phase for all the tests in this study. The rest of effluent stream passed through an activated carbon trap and vented to the hood.

At the beginning of a single fixed bed test, 1 g of sand washed in aqua regia was placed on the glass frit in the clean quartz reactor. The reactor was then placed vertically in the furnace and 1 L/min desired simulated flue gas was introduced to the reactor to acquire a baseline measurement. When a stable baseline was established, simulated flue gas was directed to vent and 50 mg of AMD solids mixed with 1 g sand treated with aqua regia was then placed on the glass frit in the quartz reactor. After that, the simulated flue gas was directed back to the reactor

with material tested and effluent mercury concentration was measured until a complete breakthrough is achieved.

3.2.2 Entrained flow system setup

Entrained flow system used in this study was comprised of the following parts: 1) sorbent feeding system, 2) simulated flue gas system, 3) entrained flow reactor, 4) mercury analyzer system. Figure 3.2 shows the schematic experimental system.

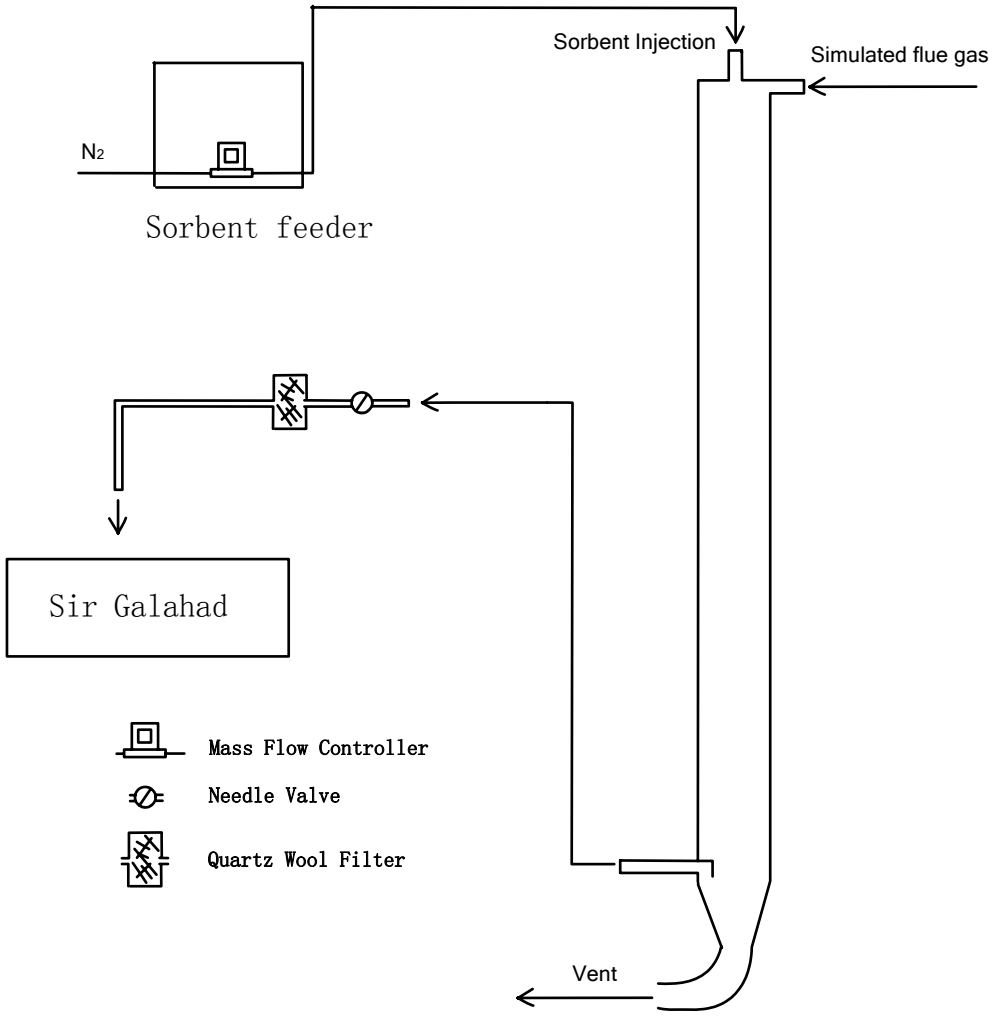

Figure 3.2. Schematic of entrained flow reactor system

A modified powder feeder (CH-1031, Sylvester and Co. Engineers, Cleveland, Ohio) was used in this study to provide the desired sorbent feeding rate. A new stainless steel screw, which has less carrying capacity of powder than the original one, was used to transport the AMD sludge material out of the sealed chamber with a N_2 carrier gas that carried the sorbent into the reactor. The rotating speed of the screw and the vibration setting of this feeder can be adjusted so that the sorbent feeding rate can be varied to accomplish a desired value. The simulated flue gas generating system and the mercury analyzer system used in entrain flow tests were the same as the ones used in the fixed bed tests.

As shown in Figure 3.2, the 2 cm ID entrained flow reactor with a total length of 65 cm was made of quartz. It was equipped with one sampling port. The reactor is designed to have a total simulated flue gas residence time of 1 second at a desired temperature. The simulated flue gas is introduced through the right port on top of the reactor and is mixed with the sorbent carried by N_2 from the top port. A flow rate of 200 ml/min of the effluent was non-isokinetically sampled from the sampling port in the reactor. The reactor was wrapped with a heating tape (Samox® insulated heating tape, Cole-Parmer Instrument Company) to be heated up to a desired temperature. The effluent sample was directed to PSA Sir Galahad system to measure total and elemental mercury concentration. In addition, a quartz wool filter wrapped with a heating tape (Fisher Scientific, Pittsburgh, PA) was added to the sample line to capture the solids that could be possibly coming out of the reactor with the sampling gas from the reactor. The rest of the simulated flue gas was vented to the hood.

An entrained flow test starts with establishing a stable baseline with a desired simulated flue gas flowing through the entrained flow reactor at a desired temperature. When a baseline is

attained, the feeder is turned on to start sorbent injection. After certain period of feeding, the feeder is turned off while mercury monitoring continued for a given period of time after that.

3.3 AMD SLUDGE MATERIAL CHARACTERIZATION

3.3.1 Particle Size Distribution Analysis

A Microtrac S3500 Tri-Laser particle analyzer (Microtrac Inc., Montgomeryville, PA) was used to analyze the particle size distribution of AMD solids. A method built in the software was used for AMD samples analysis.

3.3.2 Surface Area Analysis

The surface area of tested material was measured in the Micromeritics ASAP 2000 apparatus (Micromeritics Instrument Corporation, Norcross, GA). Brunauer-Emmett-Teller (BET) calculation was used to analyze adsorption results and calculate surface area.

3.3.3 Elemental analysis

Inductively Coupled Plasma Mass Spectrometry (ICP-MS) was used to analyze the elemental composition in the Site A sample. Fusion Inductively-Coupled Plasma (FUS-ICP) was used for the elemental analysis of Site B, Site C, Site 1, 2 and 3 samples. All the samples were sent to a commercial laboratory (Activation Laboratories Ltd, 1336 Sand Hill Drive, Ontario, USA) for analysis.

3.3.4 Foam Index Test

The air entraining admixture (AEA) is surfactant added to concrete to create fine air bubbles (< 1 mm diameter) during the mixing of the concrete. These bubbles impart freeze-thaw resistance to the concrete by providing void volume to accommodate expansion of residual water during freezing. When a fly ash contains a large amount of carbon, the carbon will adsorb AEA surfactant, which destroys the ability of the concrete to hold the required air.[40] Foam index test is a rapid method to determine the interference of a given material with the air entraining admixture requirement for concrete preparation. The Foam Index Test Procedure is conducted as following: [21, 40, 41]

1. Place 20 g of cement in a 125 mL glass jar.
2. Add 50 mL of water to the jar, then cap and shake the jar and its contents for 1 minute.
3. Add diluted AEA solution (Darex II, Grace diluted to 1:20 with DI water) in small increments of 2 to 5 drops at a time. After each addition, cap and shake the jar vigorously for 15 seconds. Observe the stability of the foam.
4. The minimum amount of diluted AEA needed to produce a foam that is stable (bubbles exist over the entire surface) for 45 seconds is the FOAM INDEX of the cement mixture.
5. Repeat steps 1 through 4 using 16 g of cement and 4 g of material tested to develop the foam index of the cement and fly ash mixture.

4.0 RESULTS AND DISCUSSION

4.1 AMD SLUDGE MATERIAL CHARACTERIZATION

4.1.1 Particle Size Distribution Analysis

A typical size distribution analysis result is shown in the figure below. The mean particle sizes of the samples in this study are listed in Table 4.1. Since all the AMD solid samples were ground and sieved with the same method, the particle size of these samples shown in Table 4.1 are similiar.

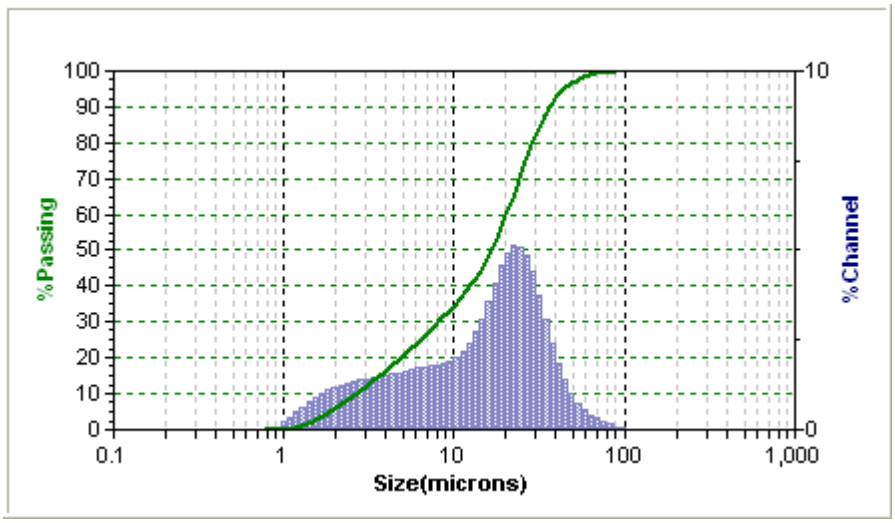

Figure 4.1. Particle size distribution of Site A sample

Table 4. 1. Mean Particle Sizes of AMD solids samples

Sample	D (μm)
Site A	18.38
Site B	9.98
Site C	21.09
Site 1	21.47
Site 2	20.27
Site 3	18.80

4.1.2 Surface Area Analysis

Six AMD sludge material samples were analyzed for surface area and the results are listed in Table 4.2. Site B shows the highest surface area among all the samples while Site 1 sample shows the lowest surface area among all the samples. Both samples are from the same site but Site B sample was acquired before lime addition. The reason resulting in such a significant difference in surface area for these samples is not clear.

Table 4. 2 Surface area of AMD sludge samples

Sample	Surface area (m^2/g)
Site A	127.7
Site B	214.6
Site C	119.1
Site 1	21.9
Site 2	102.9
Site 3	144.3

4.1.3 Elemental analysis of AMD samples

Elemental analysis of AMD samples is shown in Table 4.3. For Site A, B and C samples, Fe is the main metal existing in these AMD sludge. In general, Site A, B and C samples were produced by passive treatment technology and no lime addition process was involved. Thus, these results are in agreement with the sources description of these three samples. In Site 1, 2, 3 samples, both Ca and Fe are the dominant metals. The site description for Site 1 and 3 samples indicates the treatment method includes lime addition process, so the sludge should have certain amount of Ca, which also agrees with the elemental analysis result in Table 4.3. All the sludge samples tested in this study were dried at 110°C to remove the water content in the wet sludge.

Table 4.3. Elemental analysis results of AMD sludge samples

Sample	Fe%	Mg%	Al%	Ca%	K%	Na%	Mn%	P%
Site A	42.7	0.04	0.69	0.08	0.05	0.005	0.30	0.019
Site B	56.58	0.08	0	0.94	0.06	0.12	0.13	0.01
Site C	52.74	0.01	0.11	0.02	0.04	0.02	0.04	0.12
Site 1	2.59	0.42	0.22	34.6	0.008	0.007	0.08	0.009
Site 2	19.01	1.55	0.22	19.73	0.158	0.46	0.50	<0.04
Site 3	27.30	0.97	0.20	19.16	0.050	0.245	0.30	<0.04

4.2 MERCURY UPTAKE TEST IN A FIXED BED SYSTEM

4.2.1 Hg uptake by Site A sample in Eastern coal flue gas and PRB flue gas at 140°C

In Figure 4.2, baseline with reactor means that this baseline was established with empty reactor and simulated flue gas. Then 1 g of treated sand was placed into the reactor and the

baseline with reactor and 1 g sand was established again. As Figure 4.1 shows that the two baselines are almost identical, which indicates that the treated sand has no capacity for Hg and it does not cause any effect on Hg speciation in the reactor. Therefore, the sand used in this study can be considered as an inert material to Hg uptake and oxidation. In all of the following tests, baseline in the figure will indicate the baseline attained with reactor and 1 g treated sand inside.

Figure 4.2 shows that it took around 400 minutes to reach full mercury breakthrough at 140°C in eastern coal flue gas, while in PRB flue gas the time for breakthrough is about 1000 minutes. Percentage of oxidized Hg in the effluent is shown on the right hand axis. This percentage number was calculated as follows:

$$\text{Oxidized Hg \%} = (C_{Total} - C_{Elemental})/ C_{Total} \times 100\%$$

where, C_{Total} is the total Hg in the effluent and $C_{Elemental}$ is the elemental Hg concentration.

At the breakthrough point for both tests, about 30% of mercury in the outlet gas existed as oxidized mercury. The mercury uptake capacity for this Site A material was calculated to be 92.2 μg Hg/g in eastern coal flue gas and 174.6 μg Hg / g in PRB flue gas. The possible reason for the higher Hg uptake capacity in PRB coal flue gas will be discussed in the subsequent section.

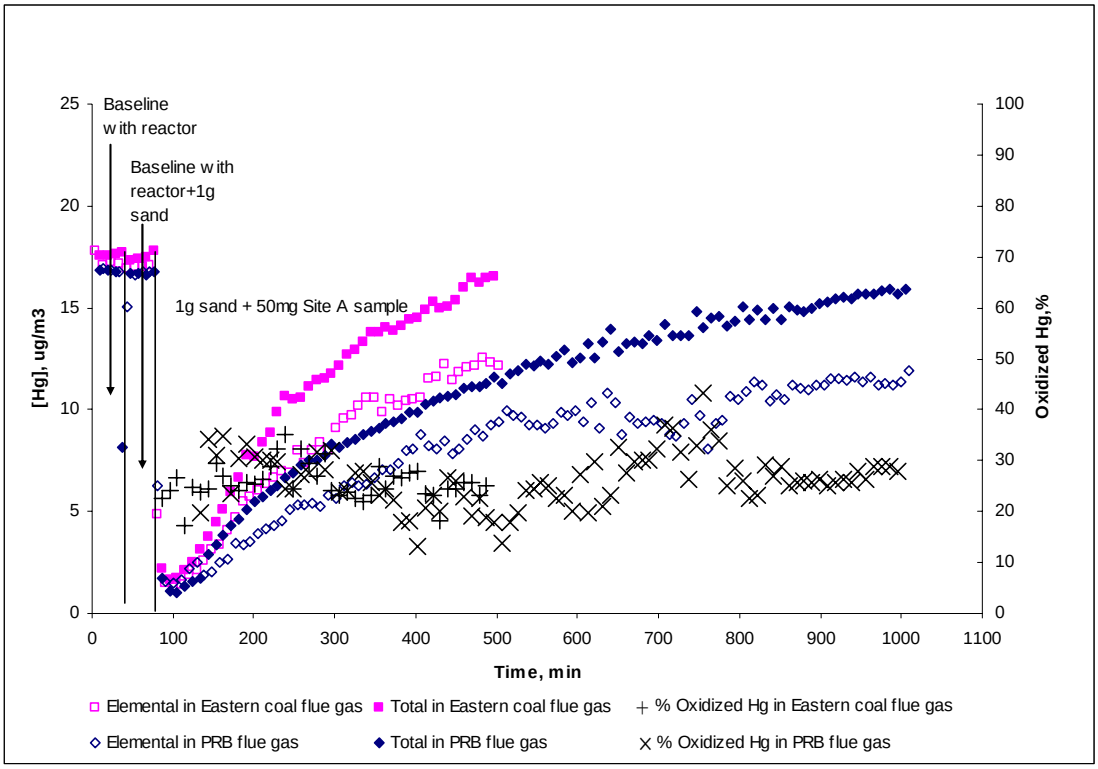

Figure 4.2. Hg uptake on Site A sample in Eastern coal and PRB flue gas at 140°C

4.2.2 Hg uptake by Site B sample in Eastern coal flue gas and PRB flue gas at 140°C

The Hg uptake test result with Site B sample in eastern coal flue gas and PRB flue gas is shown in Figure 4.3. The result shows that it took around 460 minutes to reach full mercury breakthrough at 140°C in both flue gas condition. The mercury uptake capacity for this Site B material was calculated to be 64.6 μ g Hg / g in eastern coal flue gas and 58.3 μg Hg/g in PRB flue gas. At the breakthrough point for both tests about 30% of mercury exited the reactor as oxidized mercury.

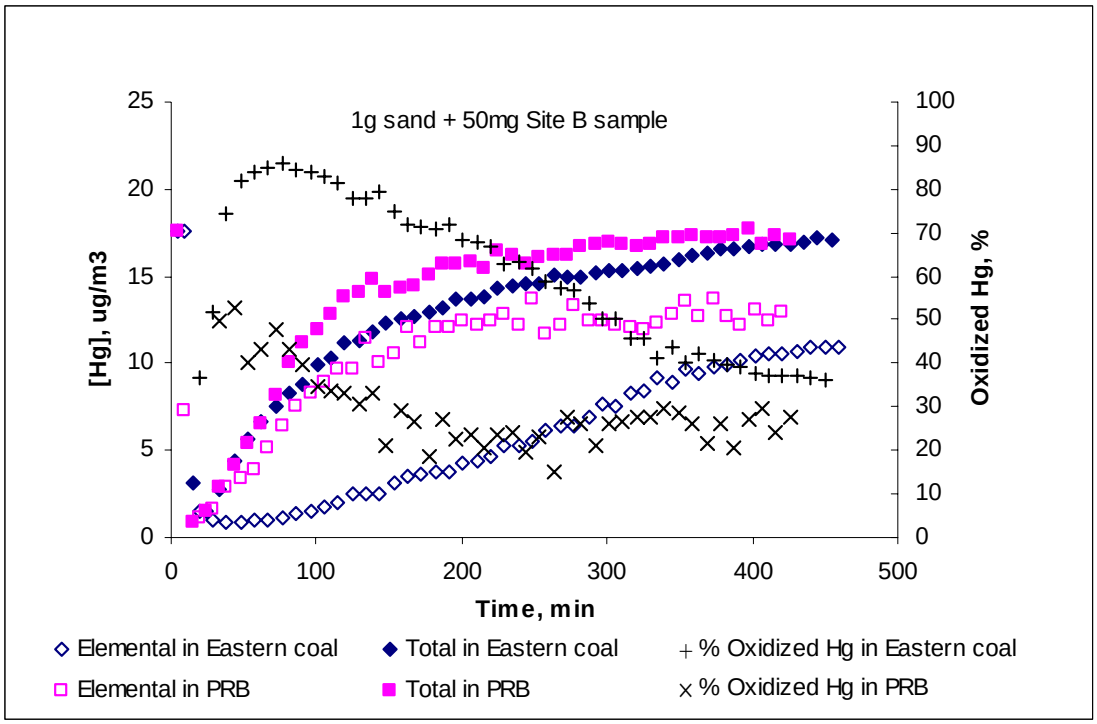

Figure 4.3. Hg uptake on Site B sample in Eastern coal and PRB flue gas at 140°C

In the test with eastern coal flue gas, the percent of oxidized Hg in effluent stream was observed to be as high as about 80% in the early test and then decreased gradually with time. In the test with PRB flue gas, about 50% of mercury existed as Hg^{2+} when leaving the reactor in the early period of the reaction, which is lower than the result in the Eastern coal flue gas. The possible reason for such behavior is not yet clear.

4.2.3 Hg uptake test on Site C sample in Eastern coal flue gas and PRB flue gas at 140°C

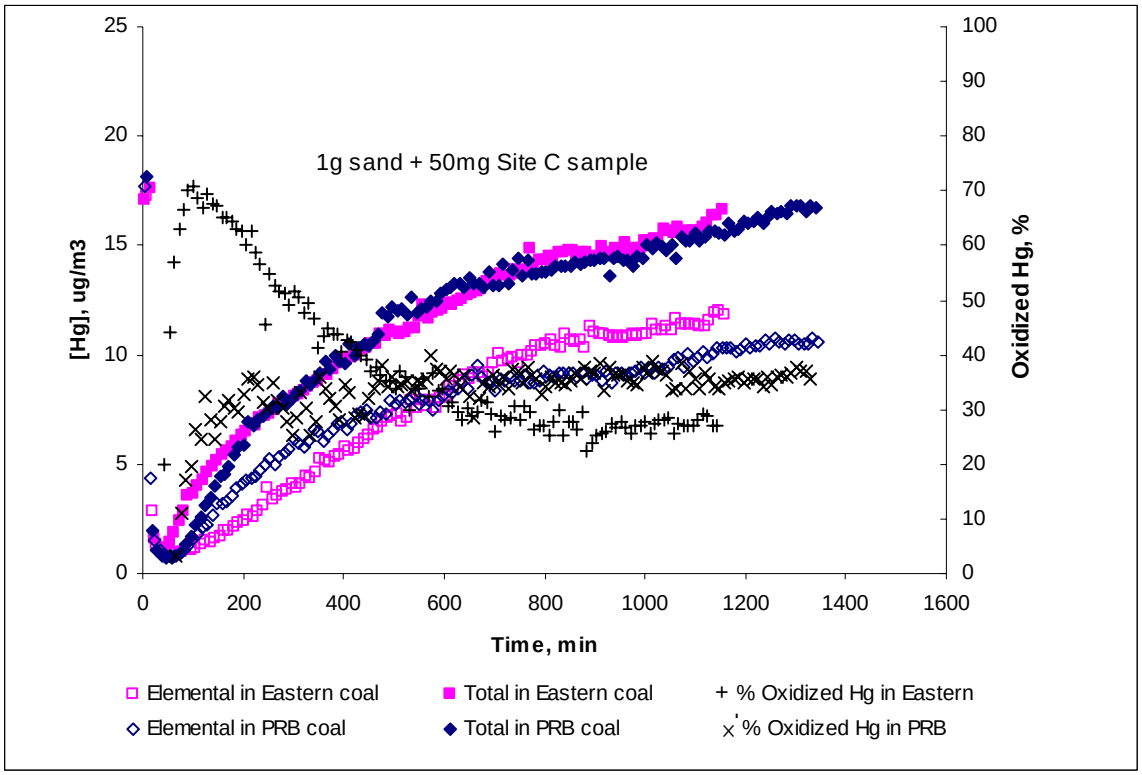

Figure 4.4. Hg uptake on Site C sample in Eastern coal and PRB flue gas at 140°C

As shown in Figure 4.4, Site C sample shows no significant difference in Hg uptake behavior in the tests with eastern coal flue gas and PRB coal flue gas. The Hg uptake capacity of Site C sample in Eastern coal flue gas and PRB flue gas is calculated to be 221.3 μg Hg/g and 232.6 μg Hg/g, respectively. When 100% breakthrough was achieved in the experiment with PRB flue gas, about 36% of Hg exited the reactor as oxidized Hg. In the test with Eastern coal flue gas, about 28% of Hg existed in the effluent as oxidized mercury after 100% breakthrough.

Table 4.4 compares Hg uptake capacity of Site A, B and C samples in the tests with Eastern coal and PRB flue gas at 140°C. Among three samples, Sample C shows the highest

capacity in Hg uptake both in Eastern coal flue gas and in PRB flue gas. Hg uptake capacity of Sample A varies from 92.2μg Hg/g in Eastern coal flue gas to 174.6μg Hg/g in PRB flue gas. Section 4.2.5 will focus on the impact of flue gas composition on Hg uptake by Site A sample at 140 °C. The possible mechanism for this will be discussed in section 4.2.5. Compared with Sample A, Sample B and Sample C did not show significantly difference in Hg uptake in the tests with these two different flue gases. With the highest 56.58% of Fe in the solids as shown in Table 4.3, Site B displays poorest capability of Hg uptake in these tests.

Table 4.4. Hg uptake capacity of Site A, Site B and C samples in Eastern coal and PRB flue gas at 140°C

Sample	Hg uptake Capacity in Eastern coal flue gas, μg Hg/g	Hg Capacity in PRB flue gas, μg Hg/g
Site A	92.2	174.6
Site B	64.6	58.3
Site C	221.3	232.6

Table 4.5 shows percent of oxidized Hg in the effluent for the tests using Site A, B and C samples with Eastern coal and PRB flue gas at 140°C after these tests achieve 100% breakthrough. As shown in Table 4.5, all three AMD solids samples show similar capability for oxidizing Hg in either Eastern coal flue gas or PRB flue gas.

Table 4.5. % Oxidized Hg with Site A, Site B and C samples in Eastern coal and PRB flue gas at 140°C

Sample	% Oxidized Hg in the test with Eastern coal flue gas	% Oxidized Hg in the test with PRB flue gas
Site A	30%	26%
Site B	37%	30%
Site C	28%	36%

4.2.4 Impact of temperature on Hg uptake by Site A sample in Eastern coal flue gas at 140°C

Due to the abundance of Site A sample for various tests, this sample was selected for the following set of experiments. Impact of temperature on Hg uptake by Site A sample is shown in Figure 4.5, where the results obtained at 140°C are compared with those obtained at 370°C. This figure clearly shows that higher temperature results in lower Hg capture, which is in agreement with the common adsorption principles. The mercury uptake capacity for Site A sample in eastern coal flue gas is calculated to be 20.5 μg Hg / g at 370°C. As shown in Figure 4.5, oxidation percentage increased from 25% to 40% when reaction temperature increased from 140°C to 370°C. Qiu et al.[29] reported that at higher temperature Fe_2O_3 nanoparticles showed increased Hg oxidation efficiency, which agrees with the findings shown in Figure 4.5. The mechanism could be that high temperature causes high activity of Site A sample as a catalyst, which could lead to high catalytic efficiency.

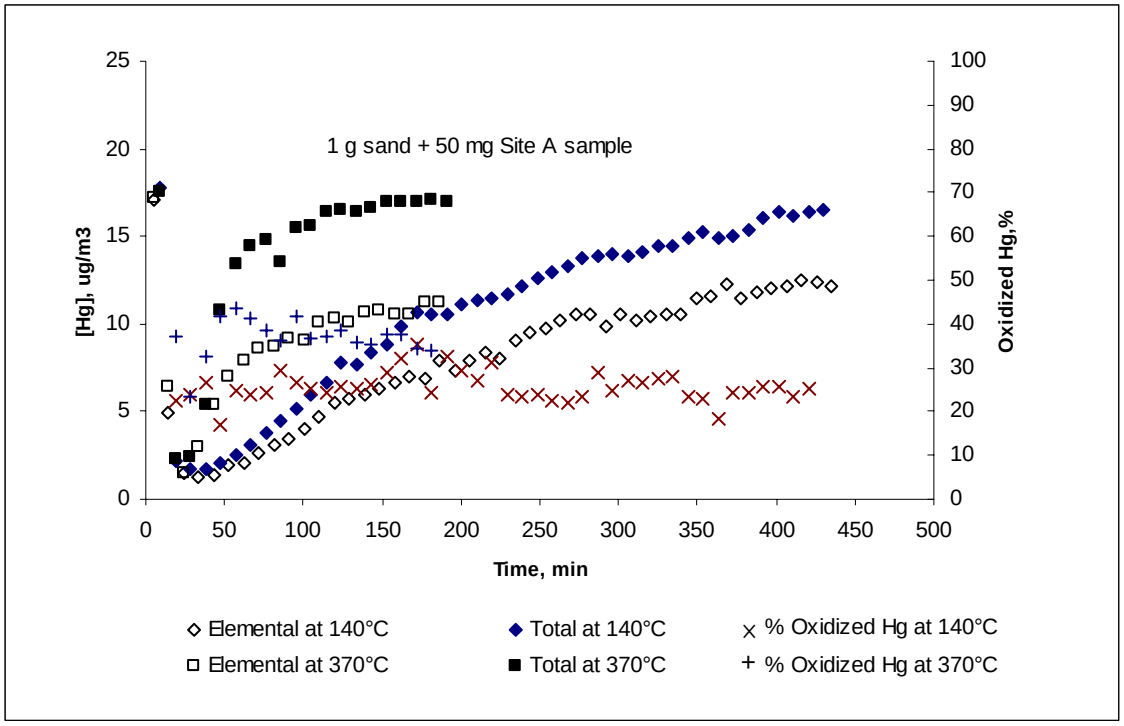

Figure 4.5. Impact of temperature on Hg uptake with Site A sample in Eastern coal flue gas at 140°C

4.2.5 Impact of flue gas composition on Hg uptake by Site A sample at 140°C

Since AMD material has never before been studied for Hg removal from coal-fired power plant flue gas, it is necessary to understand the transformation of mercury species and propose the possible mechanism of the reaction with this novel material. In this section the impact of flue gas compositions on Hg uptake and oxidation with Site A sample will be investigated. Table 4.6 shows the possible combinations of flue gas compositions in simulated flue gas.

Table 4.6. Combinations of flue gas compositions in flue gas

Number	Combinations of flue gas compositions
1	N_2+CO_2
2	N_2+CO_2+O_2
3	N_2+CO_2+ HCl
4	N_2+CO_2+ O_2+ HCl
5	N_2+CO_2+SO_2
6	N_2+CO_2+O_2+SO_2
7	N_2 +CO_2+NO_2
8	N_2 +CO_2+NO_2+O_2
9	N_2 +CO_2+NO
10	N_2 +CO_2+O_2+NO
11	N_2+CO_2+O_2+HCl+SO_2
12	N_2+CO_2+O_2+HCl+NO
13	N_2+CO_2+O_2+HCl+NO_2
14	N_2+CO_2+O_2+HCl+ SO_2+NO
15	N_2+CO_2+O_2+HCl+ SO_2+NO_2
16	N_2+CO_2+O_2+HCl+SO_2+NO_2+NO

4.2.5.1 Impact of CO_2 and O_2 on Hg uptake and oxidation at 140°C

In the baseline test with 13.5% CO_2 and balance N_2, no Hg uptake or oxidation was observed during the first 60 minutes of contact with Site A sample (Figure.4.6). After that, 6% O_2 was added into the inlet gas but there was still no Hg uptake or oxidation observed for another 60 minutes of the test. Therefore, it could be concluded that N_2, CO_2, O_2 and their combination facilitated no uptake or transformation of Hg. Such behavior indicates that physisorption of mercury in AMD solids is negligible.

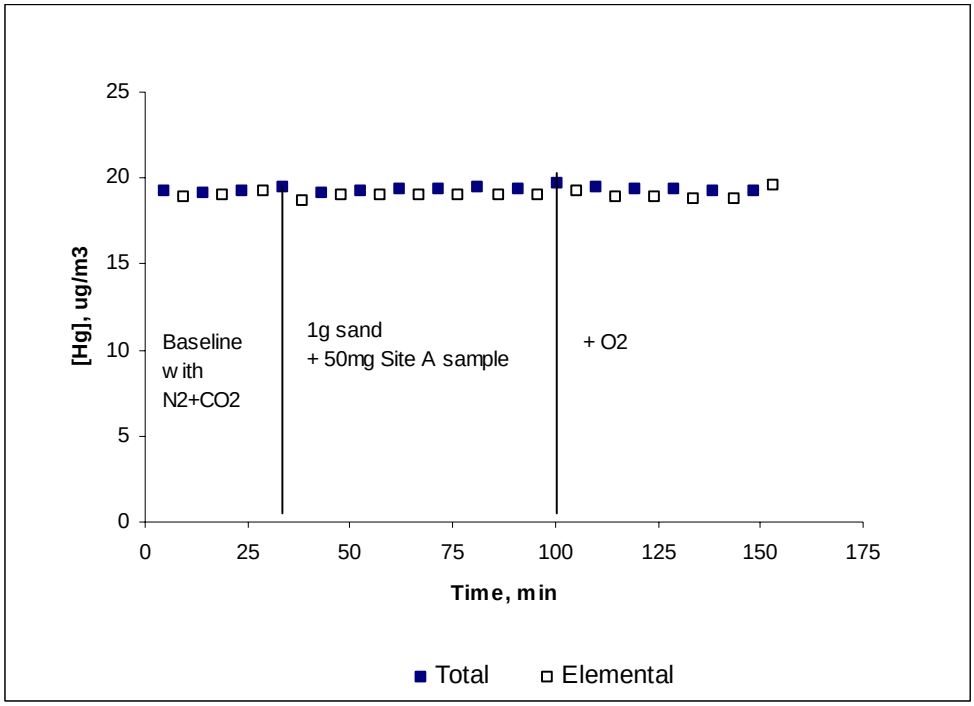

Figure 4.6. Impact of 13.5% CO_2 and 6% O_2 on Hg uptake and oxidation with N_2 at 140**°C**

4.2.5.2 Impact of SO_2 with O_2 on Hg uptake and oxidation at 140°C

Figure 4.7 shows the results of two tests elucidating the impact of SO_2 and O_2 on Hg uptake by Site A sample. In the test with N_2, CO_2 and SO_2, no Hg uptake or oxidation occurred. However, when 6% O_2 was added into the baseline in another test with 0.15% SO_2, a moderate Hg uptake was observed. It took about 60 minutes to reach 100% breakthrough and no Hg oxidation was observed under these conditions. It has already been shown that SO_2 by itself has little effects on mercury capture and oxidation on carbon-based sorbent and fly ash.[4, 20, 42] In the case of Site A sample, addition of O_2 with SO_2 results in moderate adsorption of Hg. Cao et al.[43] found that SO_2 could be oxidized in SCR reactor to SO_3 by O_2 with the SCR catalyst at about 300°C and SO_3 is responsible for Hg^0 oxidation. The proposed product of oxidized Hg is $HgSO_4$.[44] The possible mechanism responsible for the behavior in this study is that AMD Site A sample

acts as catalyst for O_2 to oxidize SO_2 to SO_3, and then Hg^0 is oxidized by SO_3. Moreover, oxidized Hg could be adsorbed on the surface of sample since there is no oxidized Hg existing in the effluent as shown in Figure 4.7. When O_2 was not involved, SO_3 could not be produced by SO_2, and then Hg^0 could not be oxidized, which is in agreement with the behavior shown in Figure 4.7.

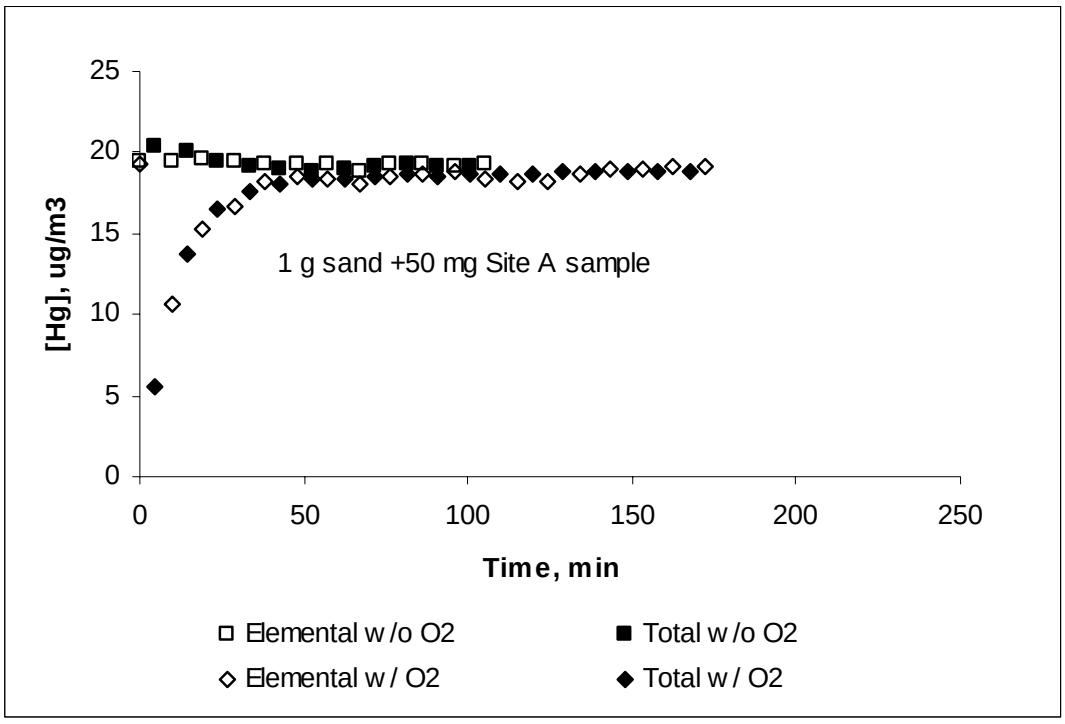

Figure 4.7. Impact of 6% O_2 on Hg uptake and oxidation with N_2, 13.5% CO_2, and 0.15% SO_2 at 140°C

4.2.5.3 Impact of HCl with O_2 on Hg uptake and oxidation at 140°C

Chen et al.[3] found that O_2 is important for the adsorption of Hg by carbon black in the presence of HCl. Figure 4.8 shows that the impact of HCl and O_2 on Hg uptake and oxidation by Site A sample. In both tests shown below (with or without O_2), addition of 50 ppm HCl led to more than 80% of Hg oxidation in effluent gas. Hg capacity was also improved compared to

experiments in the absence of HCl. The results in Figure 4.8 suggest that O_2 may not play a significant role in Hg adsorption by Site A sample in the presence of HCl as it did for carbon black. As can be seen in Figure 4.8, the presence of HCl greatly enhanced mercury oxidation. Recent study suggests that at higher temperatures (e.g. 400-700°C), the HCl is not in itself the critical chlorine-containing species that promotes mercury oxidation. Instead, it has been proposed that atomic chlorine is the primary chlorine-containing species responsible for Hg oxidation.[45] The reaction pathways leading to the formation of atomic chlorine from HCl are not well understood, although a number of possible mechanisms have been proposed.[46] Norton et al.[4] also found that the presence of HCl results in great levels of Hg oxidation for the fly ash sample with 26% of iron content, which is in agreement with the findings in this experiment.

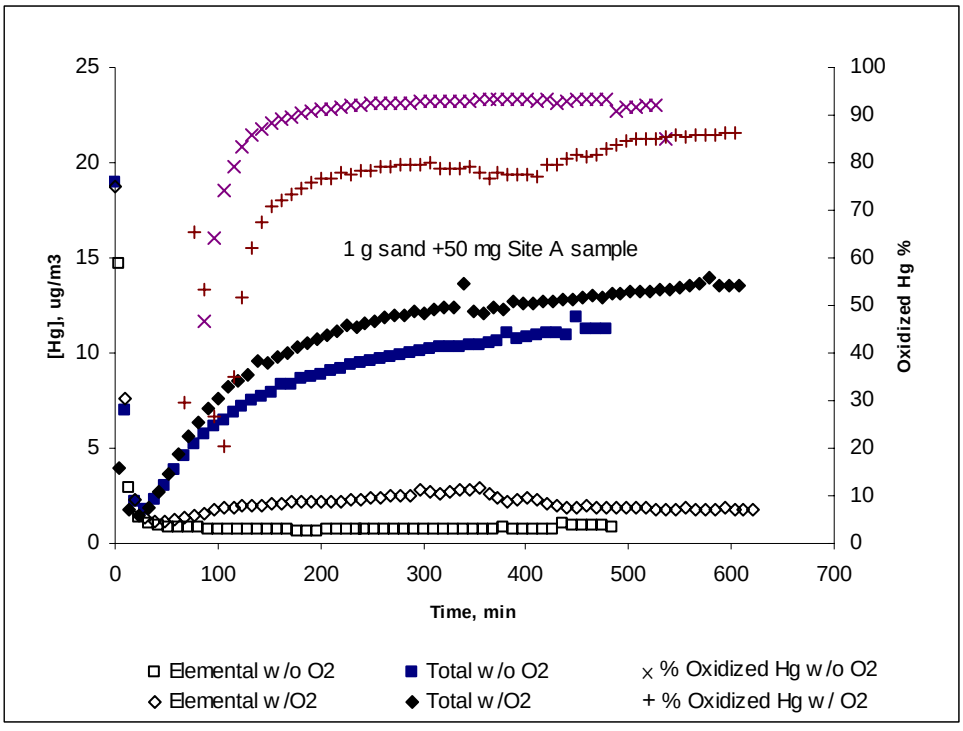

Figure 4.8. Impact of 6% O_2 on Hg uptake and oxidation with N_2, 13.5%CO_2, and 50ppm HCl at 140°C

4.2.5.4 Impact of NO_2 with O_2 on Hg uptake and oxidation at 140°C

As shown in Figure 4.9, O_2 had no effect on Hg uptake and oxidation with 20 ppm NO_2. Addition of 20 ppm NO_2 improved the Hg capacity for Site A sample as can be seen by comparing Figure 4.9 with Figure 4.6. Although no oxidized mercury was detected in the outlet stream, it can not be proved that NO_2 does not catalyze Hg^0 oxidation since the oxidized Hg could be adsorbed on the Site A sample after oxidation. NO_2 was reported to oxidize Hg^0 in the presence of fly ash and even in the absence of O_2 and HCl[4] as shown by Reactions 4 and 5 proposed by Galbreath et al.[47] and Olson et al.[48]

$$Hg\ (g) + NO_2(g) \Rightarrow HgO(s,g) + NO(g) \quad (4)$$

$$2Hg\ (g) + 5NO_2(g) \Rightarrow Hg_2O(NO_3)_2(s,g) + NO(g) \quad (5)$$

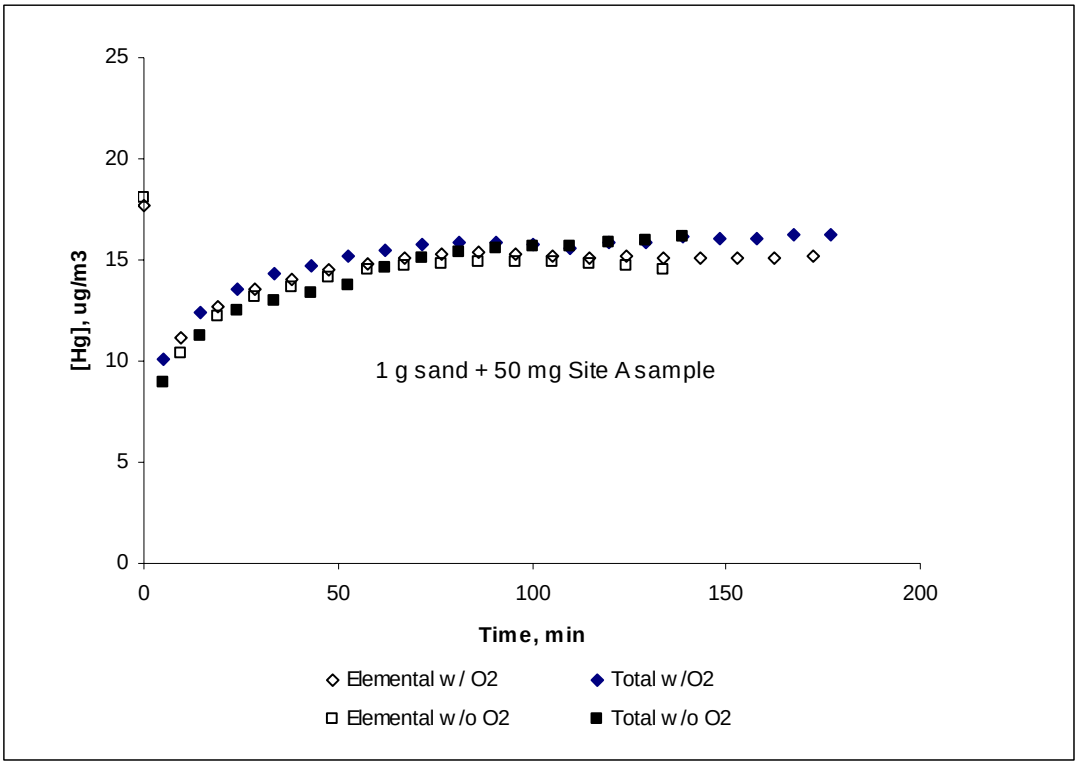

Figure 4.9. Impact of 20 ppm NO_2 on Hg uptake and oxidation with N_2, 13.5% CO_2, and 6% O_2 at 140°C

4.2.5.5 Impact of NO with O_2 on Hg uptake and oxidation at 140°C

In this experiment, 300 ppm NO was added into the gas stream with N_2 and CO_2. In the absence of O_2, NO showed no ability to promote Hg capture or oxidation by Site A solids (Figure 4.10). However, the addition of O_2 lead to Hg adsorption to a certain extent but no oxidized Hg was observed in the effluent. NO has been reported to adsorb as NO_2 onto carbon surface in the presence of O_2.[49] A possible reason for this behavior could be that certain amount of NO was transformed to NO_2 on the surface of AMD sample, which helped to adsorb Hg as discussed in Figure 4.9.

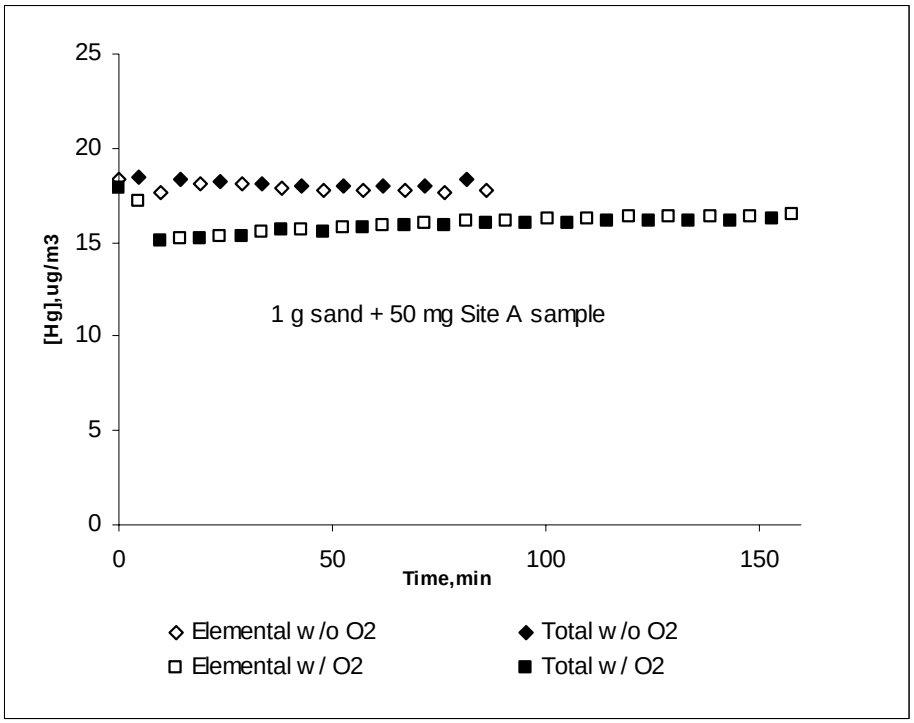

Figure 4.10. Impact of 300 ppm NO on Hg uptake and oxidation with N_2, 13.5% CO_2 and 6% O_2 at 140°C

4.2.5.6 Impact of SO_2 with HCl on Hg uptake and oxidation at 140°C

SO_2 greatly decreased adsorption capacity of activated carbon for both elemental and oxidized mercury in the presence of HCl.[50] In this section two tests were carried out to

investigate the impact of SO_2 on Hg uptake and oxidation by Site A sample in the presence of HCl. The concentration of SO_2 and HCl was 0.15% and 50ppm, respectivley. And the baseline gas composition included 6% O_2. Results in the Figure 4.11 show that SO_2 did not prohibit Hg adsorption and oxidation with HCl as it did in the case of activated carbon. After introduction of 1500 ppm SO_2 into simulated flue gas with 50 ppm HCl, Site A sample could still achieve 80% of mercury oxidation in the outlet gas. In addition, Hg capacity was not significantly affected. From this point of view, Site A sample was able to achieve higher level of performance than activated carbon in the presence of SO_2.

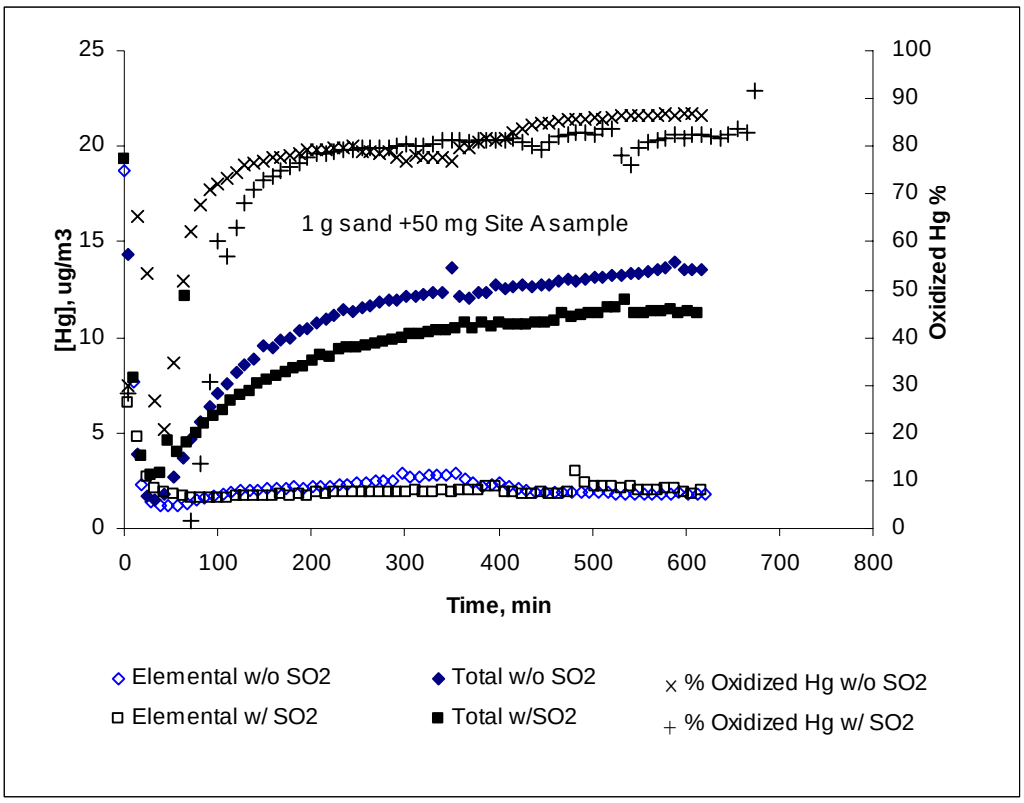

Figure 4.11. Impact of 0.15% SO_2 with on Hg uptake and oxidation with N_2, 13.5% CO_2, 6% O_2 and 50 ppm HCl at 140°C

4.2.5.7 Impact of NO_2 with HCl on Hg uptake and oxidation at 140°C

In this experiment, 50 ppm HCl and 20 ppm NO_2 was combined in the simulated flue gas and the result of this test was compared with the one conducted in the absence of NO_2 from simulated flue gas. As the figure below shows, in both tests notable Hg adsorption and 10 % oxidation were observed. NO_2 does not have distinct effect on both Hg adsorption and oxidation. It indicated that NO_2 alone did not cause negative influence on Hg uptake and oxidation caused by HCl in flue gas.

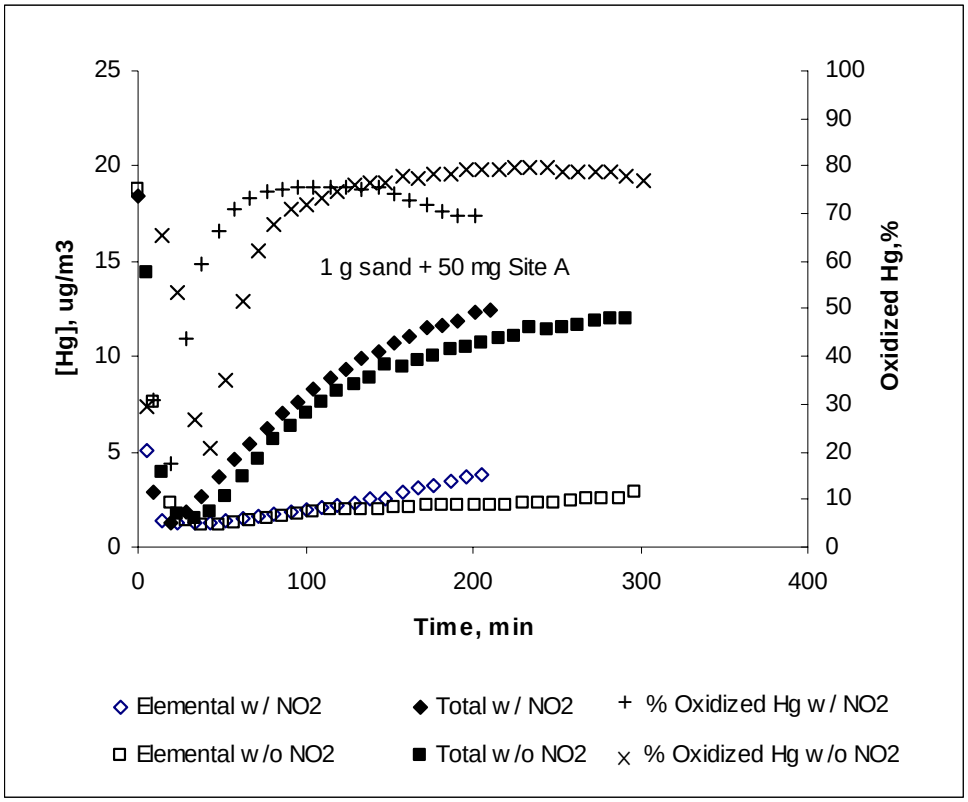

Figure 4.12. Impact of 20 ppm NO_2 on Hg uptake and oxidation with N_2, 13.5% CO_2, 6% O_2 and 50 ppm HCl at 140°C

4.2.5.8 Impact of NO with HCl on Hg uptake and oxidation at 140°C

NO was added into the baseline flue gas at a concentration of 300 ppm in the presence of 50 ppm HCl and the impact on Hg adsorption and oxidation was observed by a comparison with the tests conducted in the absence of NO. The comparison shown in Figure 4.13 reveals that the addition of NO reduced Hg adsorption capacity of this AMD material. After two hours of contact, about 41% Hg removal efficiency was observed in the presence of NO, while the test in the absence of NO yielded 62% Hg removal. Hg oxidation in both tests was remarkable as evidenced by the presence of about 80% of Hg^{2+} in the outlet stream. NO seems to help oxidize Hg from the beginning of the experiment, but this cannot be verified due to the possibility that the enhancement could be caused by desorption of Hg^{2+} absorbed on the surface of material in the presence of NO. These results reveal that NO could moderately reduce Hg adsorption capacity of AMD material in the presence of HCl. However, Hg oxidation was not significantly affected.

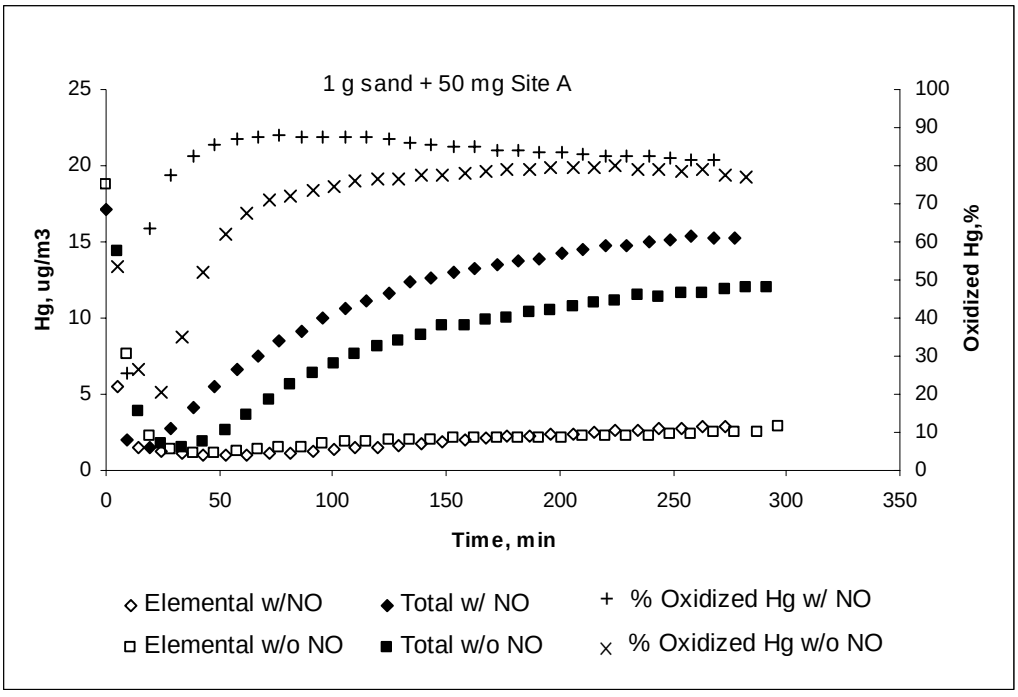

Figure 4.13. Impact of 300ppm NO on Hg uptake and oxidation with N_2, 13.5% CO_2, 6% O_2 and 50 ppm HCl at 140°C

4.2.5.9 Impact of NO_2 and NO on Hg uptake and oxidation with flue gas comprised of N_2+CO_2+O_2+HCl+SO_2

In previous research, SO_2, NO and NO_2 combined individually with HCl were not found to affect Hg adsorption and oxidation remarkably. Therefore, HCl, SO_2 and NO combination and HCl, SO_2, NO_2 combinations were used in the following two experiments to study their simultaneous impact on Hg adsorption and oxidation. These test results were compared with full flue gas Hg uptake test in Figures 4.14 and 4.15.

When NO_2 was eliminated from the simulated flue gas, HCl, SO_2 and NO combination helped AMD material attain about 76% of oxidized Hg in effluent gas stream after 2 hours of reaction (Figure 4.14). In contrast, Hg uptake test in a full flue gas was only about 25%. This result suggests that NO_2 removal from the flue gas should play important role by adversely inpacting Hg oxidation under these conditions.

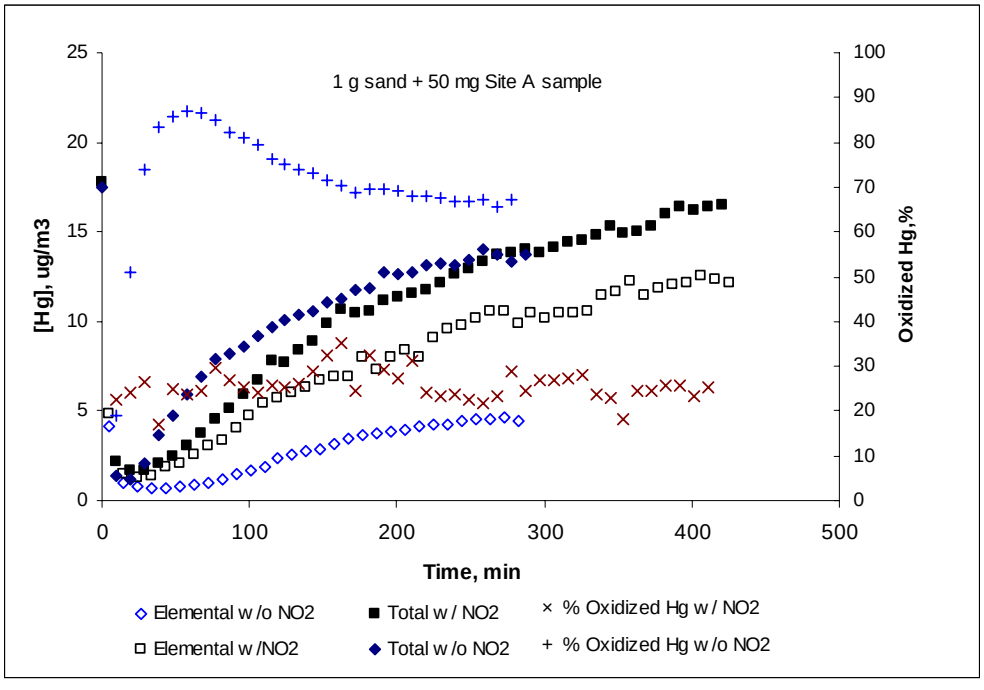

Figure 4.14. Impact of 20 ppm NO_2 on Hg uptake and oxidation with N_2, 13.5% CO_2, 6%O_2, 0.15% SO_2, 300 ppm NO and 50 ppm HCl at 140°**C**

In Figure 4.15, the result with HCl, SO_2 and NO combination in flue gas shows great similarity with the test result in simulated flue gas including all gas compositions. Many of elemental Hg data points are almost overlapped in the figure. After 2 hrs of contact, the Hg removal efficiency and percent of oxidized Hg in effluent for two tests are about 51%, 39% and 57%, 25%, respectively. This result shows that absence of NO from the flue gas comprised of HCl, SO_2, and NO_2 does not lead to distinct impact on Hg adsorption and oxidation by AMD material. Therefore, the results in both Figures 4.14 and 4.15 suggest that NO_2 and SO_2 are the most crucial gas combination on Hg oxidation due to the behavior observed in Figure 4.14.

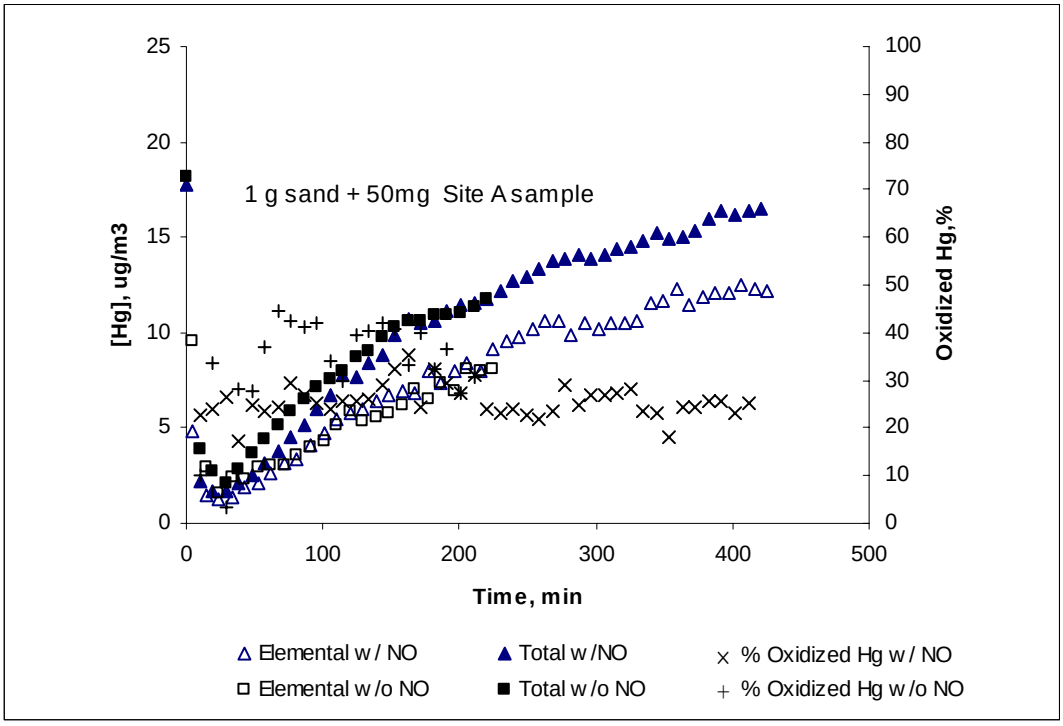

Figure 4.15. Impact of 300 ppm NO on Hg uptake and oxidation with N_2, 13.5% CO_2, 6% O_2, 0.15% SO_2, 20 ppm NO_2 and 50 ppm HCl at 140°**C**

A synergistic effect between NO_2 and SO_2 was noticed in different studies on Hg oxidation and adsorption.[4, 38] A mechanism was proposed to explain the effect of NO_2 and SO_2 on adsorption/oxidation of Hg^0 by activated carbon,[1] This mechanism proposes that HCl, SO_2 could be bound to the basic sites on the surface. As an electron sink NO_2 could accept electrons transferred from elemental mercury, which resulted in Hg^0 oxidation to form oxidized Hg. These oxidized Hg species, such as Hg^{2+}, $HgCl_2$ can be also bound to basic sites. When these binding sites are used up, Hg capture will stop and breakthrough occurs. SO_2 could occupy these sites as sulfate so that oxidized mercury can not be bound any longer. This mechanism is proposed on the surface of carbon. However, the combined effect of NO_2, HCl and SO_2 on mercury oxidation and adsorption for this AMD material also follows this theory. This agreement could suggest that this model is suitable for both carbon surface and the surface of this AMD material.

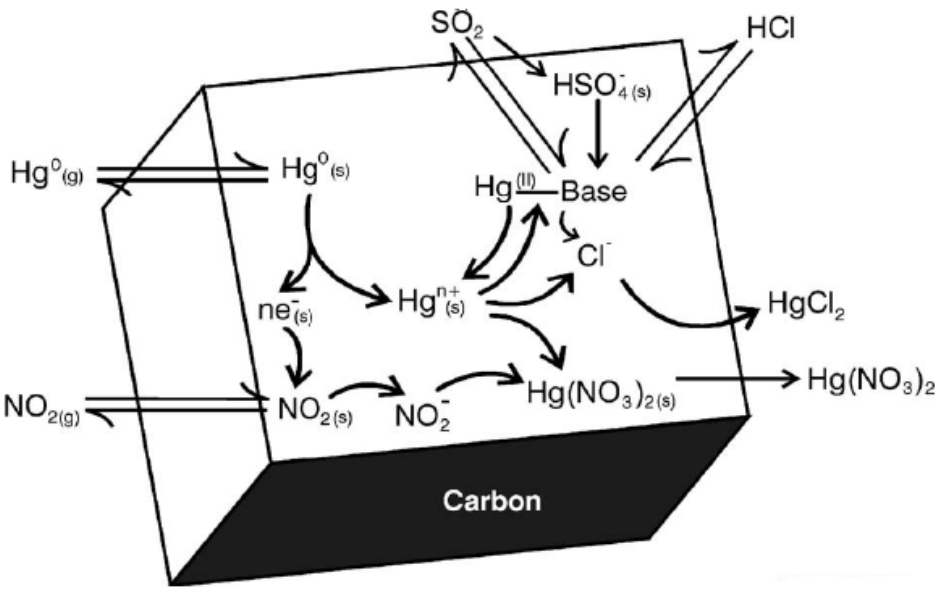

Figure 4.16. Suggested heterogeneous model for mercury capture showing potential impact of SO_2 and NO_2[1]

Table 4.5 shows the Hg removal efficiency and percent oxidized mercury in the effluent from the reactor ([Hg^{2+}] / inlet [Hg]) after 2 hrs of contact with different flue gas compositions. This table indicates that NO_2 and NO did not affect Hg oxidation by AMD sludge material when they are combined with HCl individually or simultaneously in flue gas. Combination of SO_2, HCl and NO showed similar behavior. However, combination of SO_2, HCl and NO_2 shows significant negative impact on Hg oxidation. Dunham et al.[20] suggested a heterogeneous model for mercury capture explaining potential impact of SO_2 and NO_2 as shown in Figure 4.16.

However, this model is proposed for carbon surface. The mechanisms responsible for the observations in this research are not clear. As the Table 4.7 shows, when NO is added into flue gas with HCl or combination of HCl and SO_2, Hg removal efficiency is 41.6% or 46.3% (vs. 62.2% in HCl). Therefore, NO shows inhibitory effect on Hg adsorption not only by itself but also with combination of HCl and SO_2, Miller et al.[38] reported an increase in mercury uptake capacity of activated sorbent when adding NO to the flue gas. The test result with AMD sludge material was contradicted with these findings but the mechanisms are still unclear.

Table 4. 7. Hg removal efficiency and outlet [Hg^{2+}] / inlet [Hg] after 2 hrs of contact with different flue gas compositions in fixed bed tests with Site A sample at 140°C

Flue gas compositions	Hg removal efficiency	Outlet [Hg^{2+}]/inlet [Hg]
N_2+CO_2+O_2	0	0
N_2+CO_2+O_2+SO_2	4.7%	0
N_2+CO_2+O_2+NO_2	11.1%	0
N_2+CO_2+O_2+NO	10.8%	0
N_2+CO_2+O_2+HCl	62.2%	79%
N_2+CO_2+O_2+HCl+SO_2	65.5%	78.4%
N_2+CO_2+O_2+HCl+NO	41.6%	86.9%
N_2+CO_2+O_2+HCl+NO_2	57.5%	75.5%
N_2+CO_2+O_2+HCl+ SO_2+NO	46.3%	76.2%
N_2+CO_2+O_2+HCl+ SO_2+NO_2	51.9%	39.5%
N_2+CO_2+O_2+HCl+SO_2+NO_2+NO	57.2%	25.6%

4.3 MERCURY UPTAKE BY AMD SOLIDS IN ENTRAINED FLOW SYSTEM

In this section, Site A, Site 1, Site 2 and Site 3 samples were injected into the entrained flow system at certain injection rate to test their ability for Hg removal and oxidation in eastern coal and PRB coal flue gas at 140°C. The effect of temperature and injection rate on Hg removal by the injection of Site A sample was also investigated in this section. In addition, removal efficiency of AMD Site A sample in the entrained flow system was compared with the performance of commercial powdered activated carbon (FGD Activated carbon, Norit America, Marshall, TX)

4.3.1 Impact of quartz wool filter on mercury measurement in the entrained flow reactor

As mentioned in Section 3.2.2, a quartz wool filter was used in the sampling system to capture the possible sorbent carried out by the sampling gas stream, and eliminate interference with mercury measurements. On the other hand, the sorbent possibly captured in the filter may have impact on the mercury species transformation in the sampling gas directed into Sir Galahad. Therefore, it is necessary to evaluate if this glass wool filter interferes with mercury measurement. In this test, Site A sample was injected with the sorbent loading of 0.39 g/m^3 in the simulated Eastern coal flue gas. After about 50 minutes, injection was stopped by turning off the powder feeder. As shown in Figure 4.17, mercury concentration in the sampling gas began to increase with the time after injection stopped. This behavior was unexpected since no sorbent was injected into the reactor and mercury concentration in the sampling gas should recover to the same level as that in the inlet simulated flue gas. In order to eliminate the possibility that quartz wool filter possibly containing sorbent affected mercury measurement, quartz wool filter in this

test was removed from the sampling system after about 150 minutes of the test. Then the sampling system was reconnected without the filter and the mercury measurement continued. As can be seen in Figure 4.17, mercury concentration was identical to that with glass wool filter in line. Based on these and the fact that there was no discoloration of glass wool, it can be concluded that quartz wool filter used in sampling system has no impact on mercury measurement.

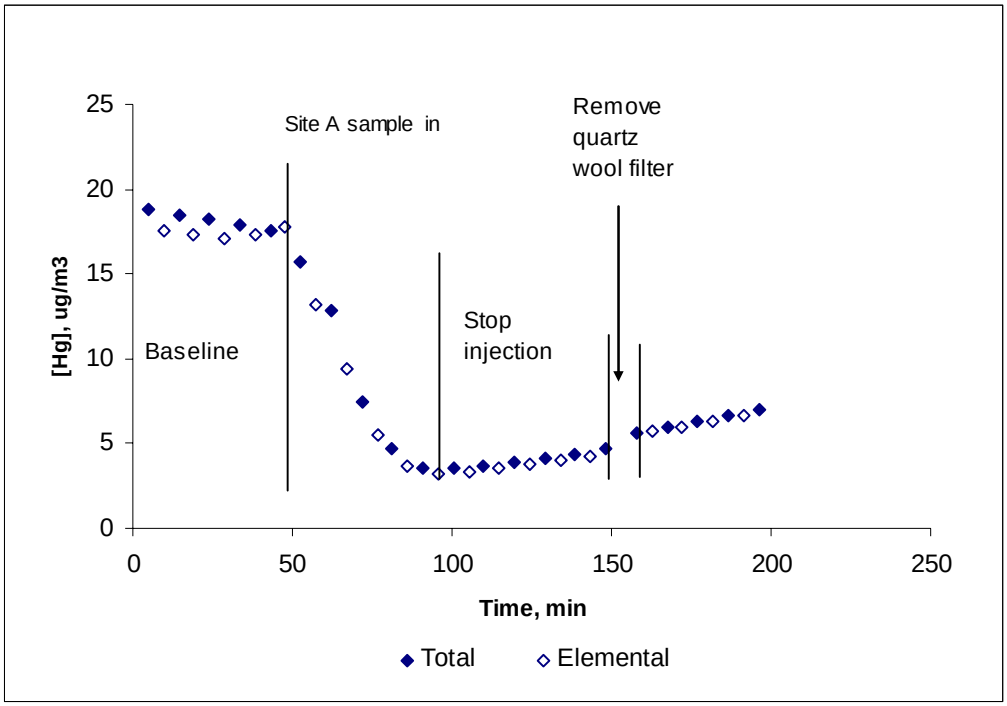

Figure 4.17. Impact of quartz wool filter on mercury measurement in entrained flow reactor

4.3.2 "Reactor effect" on mercury measurement in the entrained flow reactor

Figure 4.17 shows that mercury concentration in sampling gas is slowly increasing after sorbent injection stopped. However, this recovery process is slow (after ceasing injection for 100 minutes, the Hg concentration in effluent recovers to only about half level of inlet Hg

concentration). Similar observation was also found in other research.[51] Wu et al.[51] suggested that this phenomenon is the result of sorbent sticking to the wall of the reactor or sorbent accumulating in the horizontal duct of the reactor so that the contact time of sorbent with flue gas is longer than the calculated residence time in the reactor. In order to identify the reason for this behavior, the following test was conducted: Site A sample was injected in the entrained flow reactor with the sorbent loading of 0.39 g/m^3 in PRB flue gas. Fifty minutes after injection stopped, the simulated flue gas was directed to bypass the reactor and mercury concentration in the inlet flue gas was measured as shown in Figure 4.18 as "Baseline bypassing reactor". As shown in Figure 4.18, baseline bypassing reactor is at the identical level as the baseline. Such result indicates that sampling system causes no interference with the mercury measurement. After bypassing reactor for about another 50 minutes, simulated flue gas was redirected to the entrained flow reactor and the sampling system was reconnected. Figure 4.18 shows that mercury removal was still achieved at about 50% when the simulated flue gas was introduced in the reactor with no sorbent injection. Such observation confirms that mercury is still being removed by the reactor even without any sorbent injected. This phenomenon is named in this study as "reactor effect" and it is most likely due to sorbent attached to the reactor surface.

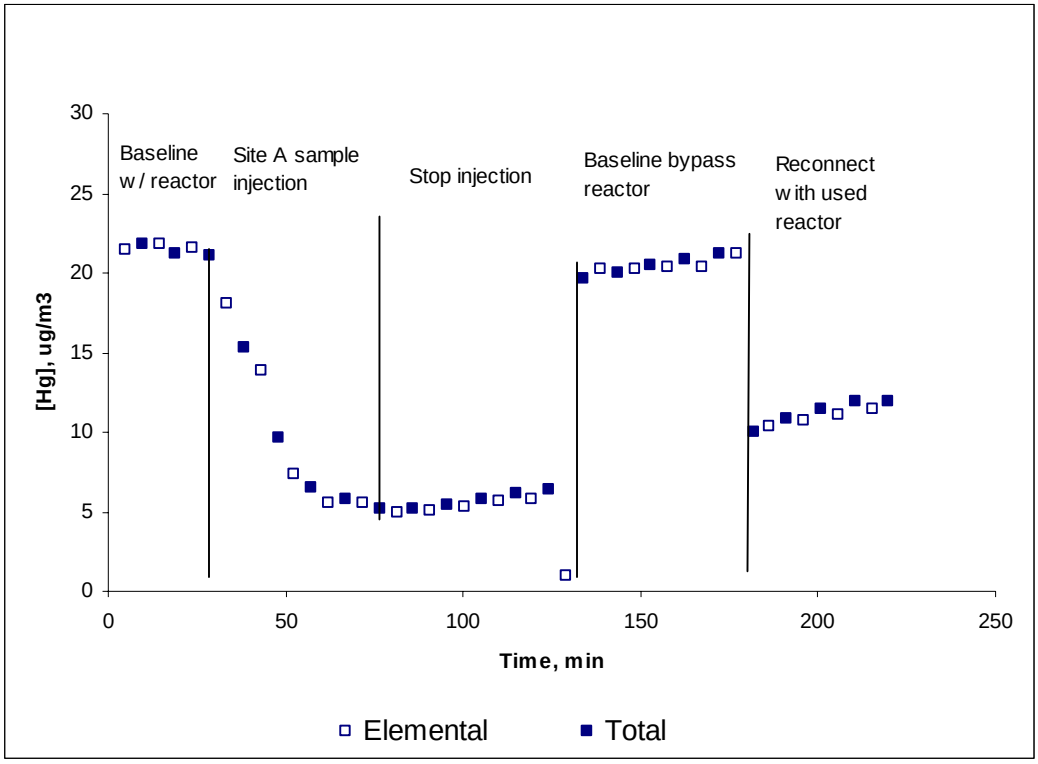

Figure 4.18. "reactor effect" on mercury measurement in entrained flow reactor

After the test in Figure 4.18, the reactor was washed with DI water and the deposited material was collected in a beaker and filtered through a filter paper with 0.45μm pore size. After filtration, the filter paper was heated in an oven at 110℃ for 1 hr and the weight difference is denoted as the mass deposited on the reactor wall. This test revealed a total of 0.0031 g of sorbent deposited in the reactor. Assuming that mercury removal in the reactor in the absence of sorbent injection is caused by these deposits, if follows that the adsorption capacity of these deposits is 5,900μg/g, which is significantly higher compared with the sorbent capacity in other studies.[10, 17, 24, 52, 53] Further research is needed to investigate the mechanism for this observation.

4.3.3 Impact of flue gas composition on mercury removal by AMD Site A sample in the entrained flow reactor.

In this test, Site A solids feeding rate provided by modified powder feeder was set at 0.29 g/hr, which resulted in sorbent loading in the simulated flue gas of 0.39 g/m^3 and the sorbent to Hg ratio of about 22,100. As shown on Figure 4.19, the total and elemental Hg concentration in both Eastern coal and PRB coal flue gas approached steady-state values after about 50 minutes of AMD injection. When Hg removal was at about 80% and no obvious Hg oxidation was observed in this experiment. Such behavior could be explained by the fairly short residence time in the reactor. No obvious difference in Hg removal under these two flue gase conditions was observed in the entrained flow tests. As observed in fixed bed tests, there was no difference in Hg adsorption and oxidation with this AMD sample in simulated eastern coal and PRB flue gas during the first several minutes of fixed bed tests. The residence time in the entrained flow reactor was only 1 second and the effect of flue gas composition on Hg removal could not be displayed in such short residence time.

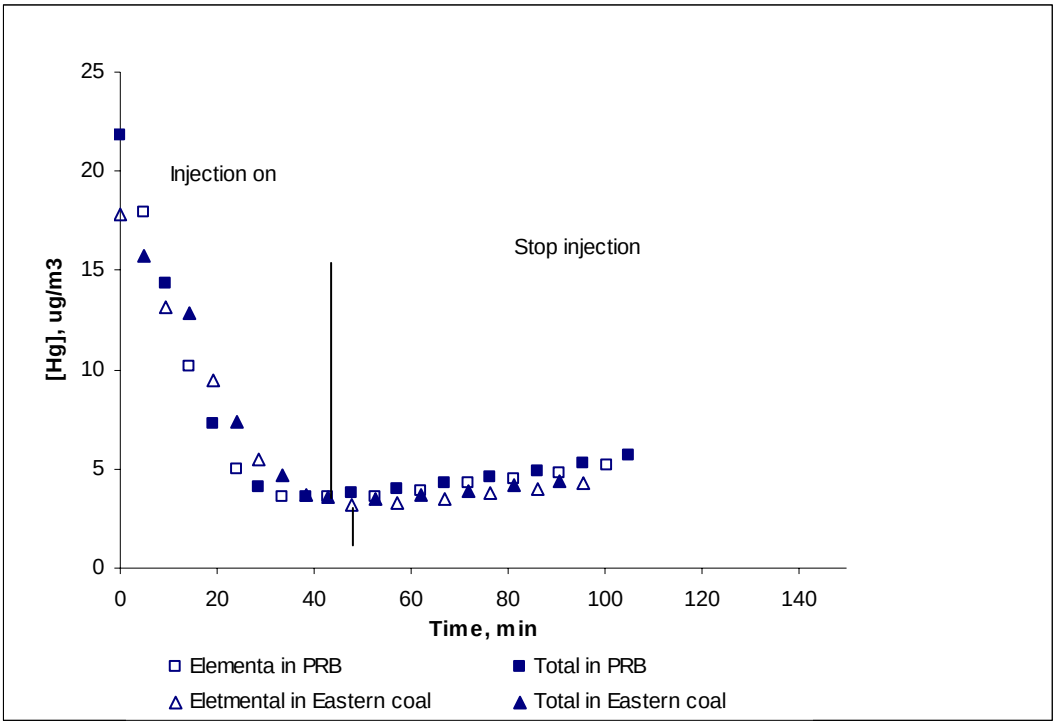

Figure 4.19. Hg removal in entrained flow test with Site A sample at 140℃ in PRB and Eastern Coal flue gas

4.3.4 Impact of temperature on mercury removal by Site A sample in the entrained flow reactor

Site A sample was injected in the entrained flow reactor under identical conditions but at two different temperatures of 140 °C and 370°C. The results of two tests are compared in Figure 4.20. After reaching steady state, Hg removal efficiency with Site A sample was about 80% at 140°C and 58% at 370°C in eastern coal flue gas. This figure clearly shows that lower temperature results in higher Hg capture in entrained flow test, which agrees with the common adsorption principles and the fixed bed test results discussed in Section 4. 2. Mercury uptake by Site A sample is also occurring by chemisorptions as evidenced by significant impact of HCl discussed in Section 4.2.

High temperature could increase the chemiadsorption rate. However, due to the quite short residence time in this reactor, chemisorptions of mercury on AMD solids may not be displayed as clearly as the test in fixed bed system.

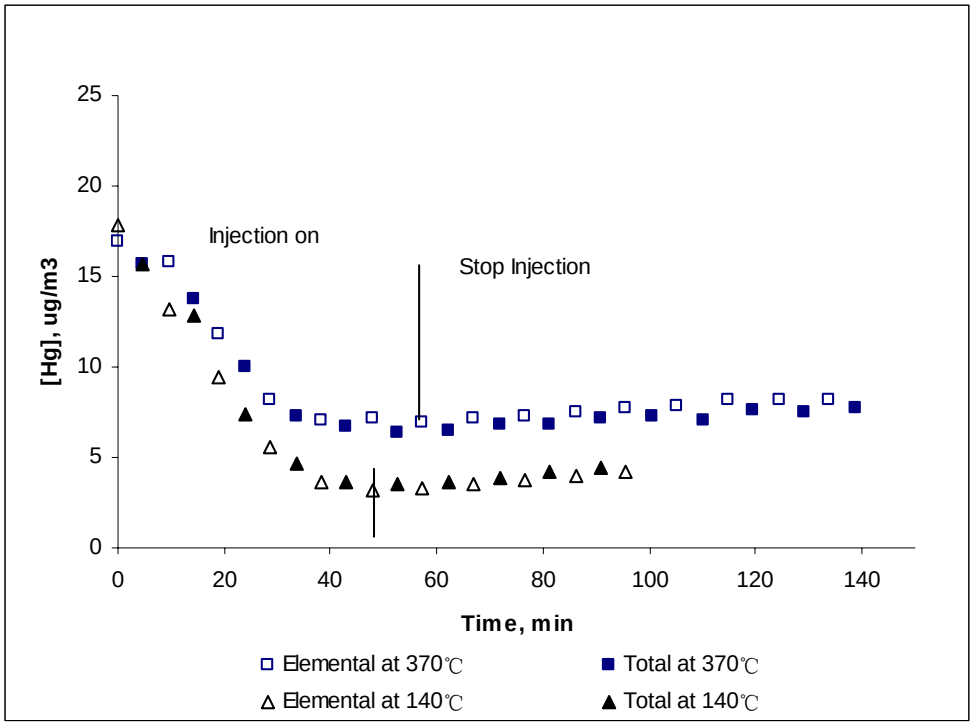

Figure 4.20. Hg removal in entrained flow test with Site A at 140℃ and 370℃ in Eastern Coal flue gas

4.3.5 Impact of injection rate on mercury removal by Site A sample in the entrained flow reactor

In order to investigate the effect of Site A sample injection rate on Hg removal in the entrained flow system, Site A sample was injected at two different rates, namely 0.29 g/hr and 0.56 g/hr. The sorbent loading in the simulated flue gas was 0.3 g/m^3 and 0.76 g/m^3 respectively, and the ratio of sorbent / Hg was about 22,100 and 43,000, respectively. The test result with these injection rates in eastern coal flue gas are compared in Figure 4.21. Figure 4.21 shows that the steady state at higher

injection rate was achieved a bit earlier (35 minutes versus 45 minutes). Also Hg removal efficiency at higher injection rate was higher (95% vs 80%). These encouraging results indicate that higher Site A injection rate can help achieve higher Hg removal performance in the entrained flow test.

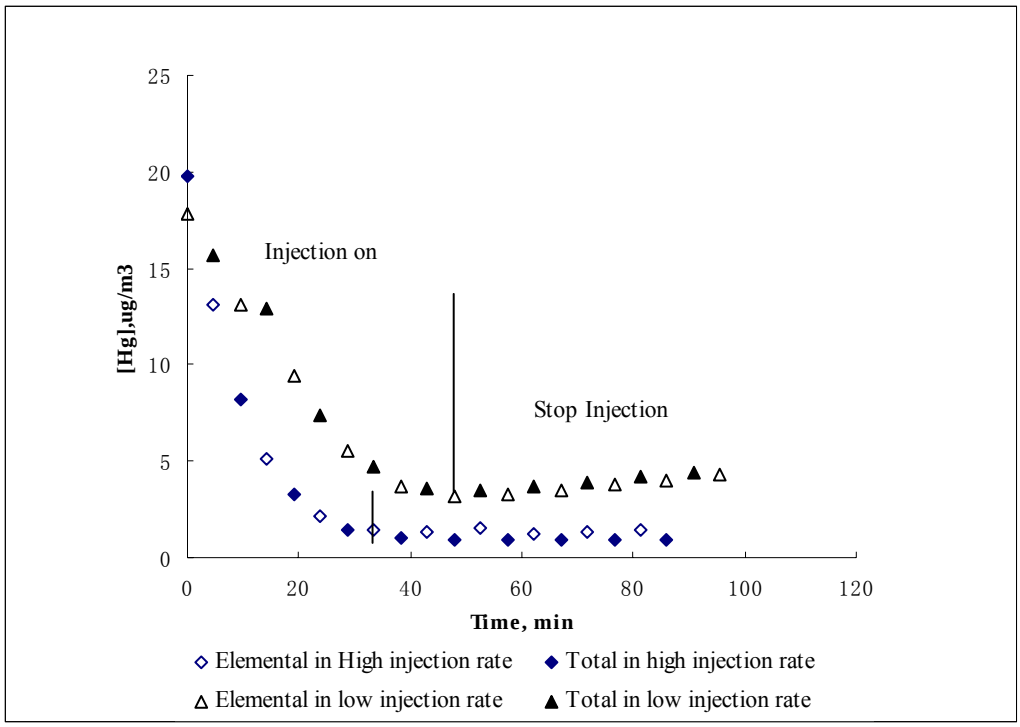

Figure 4.21. Hg removal in entrained flow test with Site A at injection rate of 0.76g/m^3 and 0.39g/m^3 in Eastern Coal flue gas

4.3.6 Comparison of Site A sample to commercial FGD activated carbon in Eastern coal flue gas at 140 °C

Commercially available FGD activated carbon was injected at 140°C in eastern coal flue gas at the injection rate of 0.19 g/hr, resulting in activated carbon load in simulated flue gas of 0.26 g/m^3 and the ratio of activated carbon/Hg of 14480. The surface area of FGD activated carbon used in this test is 600 m^2/g. Performance of FGD carbon is compared with the performance of Site A sample in

Figure 4.22. It can be seen that FGD activated carbon injection took about 15 minutes to reach steady state Hg removal. Compared with Site A injection test, less time was required for the system performance to reach the steady-state behavior with FGD activated carbon and the final Hg removal efficiency was almost 100%. In industrial PAC injection the injection rate of activated carbon varies between 1 and 10 lb/MMacf,[17] which is equivalent to 0.016 g/m^3 and 0.16 g/m^3. This result shows that about 30% lower injection rate of FGD activated carbon in this entrain flow test resulted in about 30% higher Hg removal efficiency and shorter time to achieve steady state. It indicates that the capability of Hg removal with Site A material is lower than the one with FGD activated carbon.

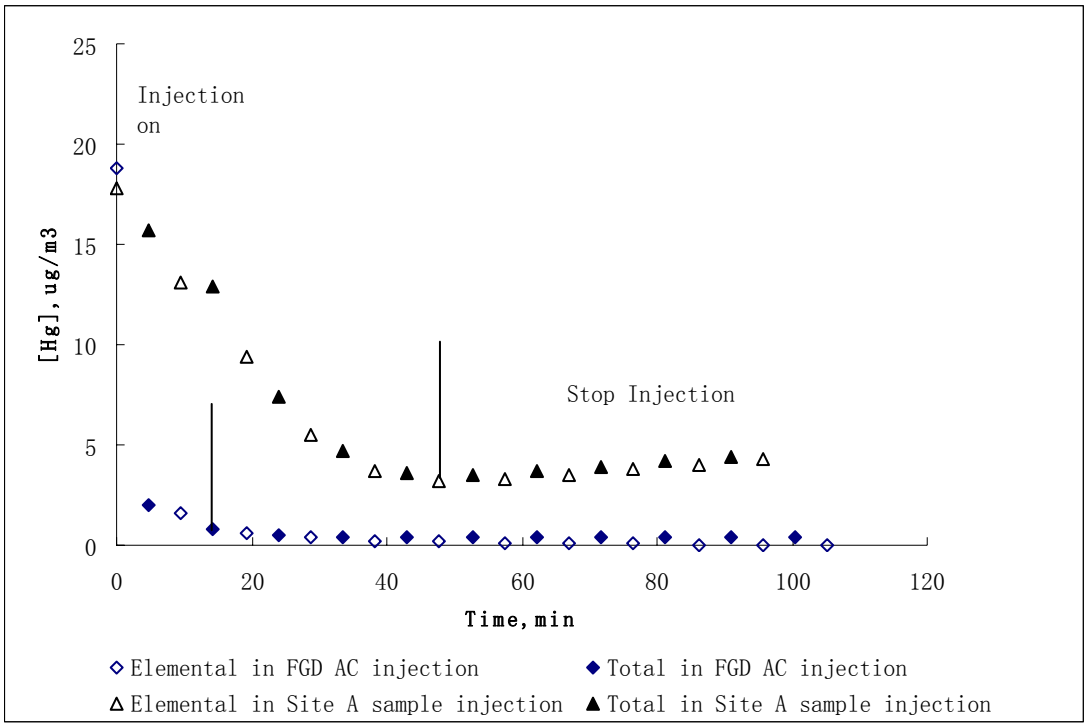

Figure 4.22. Hg removal in entrained flow test with Site A sample and FGD activated carbon at 140 °C in Eastern Coal flue gas

4.3.7 Entrained flow tests with other AMD samples in Eastern coal and PRB flue gas at 140°C

AMD sludge samples from Site 1, Site 2 and Site 3 sample were injected into the entrained flow reactor in PRB and Eastern coal flue gas at 140°C. The feeding rate of AMD solids varied between 0.30 g/hr and 0.34 g/hr to yield the ratio of sorbent and Hg between 22,860:1 to 25,910:1. The test results for these AMD sorbents are compared in Figures 4.23~4.25. Figure 4.25 shows that Site 1 sample displayed the lowest Hg removal efficiency in the entrained flow test among these 3 AMD sorbents. At steady-state, Hg removal efficiency with Site 1 injection was about 26% at 140°C in both Eastern coal and PRB flue gas conditions.

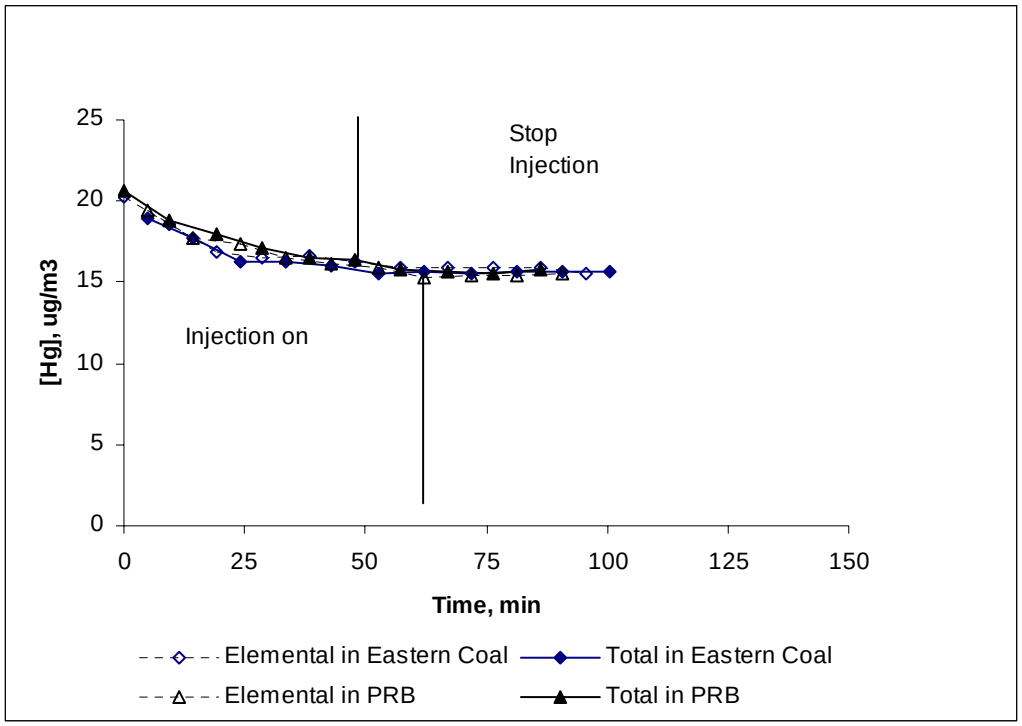

Figure 4.23. Entrain flow test results with Site 1 sample in Eastern coal and PRB flue gas at 140℃

Injection of Site 2 and Site 3 sample resulted in about 45% ~ 55% Hg removal in the entrained flow tests shown on Figure 4.24 and Figure 4.25, respectively. In Eastern coal flue gas and PRB flue gas conditions, no significant difference in Hg removal efficiency was observed in PRB or Eastern coal flue gas. In addition, no Hg oxidation was observed in these tests, which is in agreement with previous entrained flow tests with Site A sample.

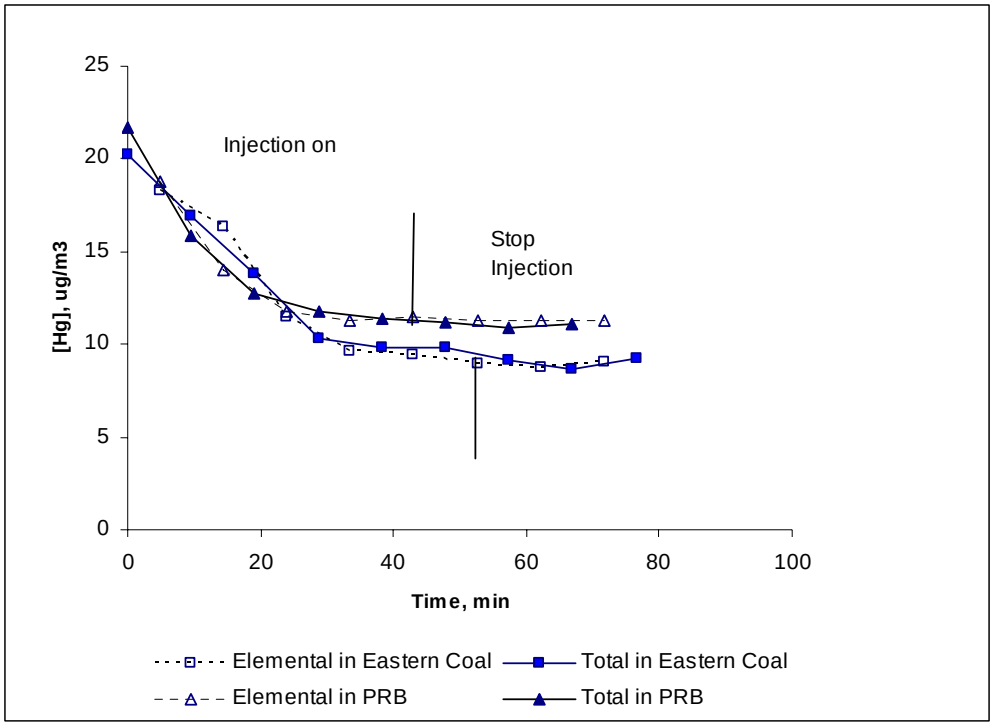

Figure 4.24. Entrained flow test results with Site 2 sample in Eastern coal and PRB flue gas at 140℃

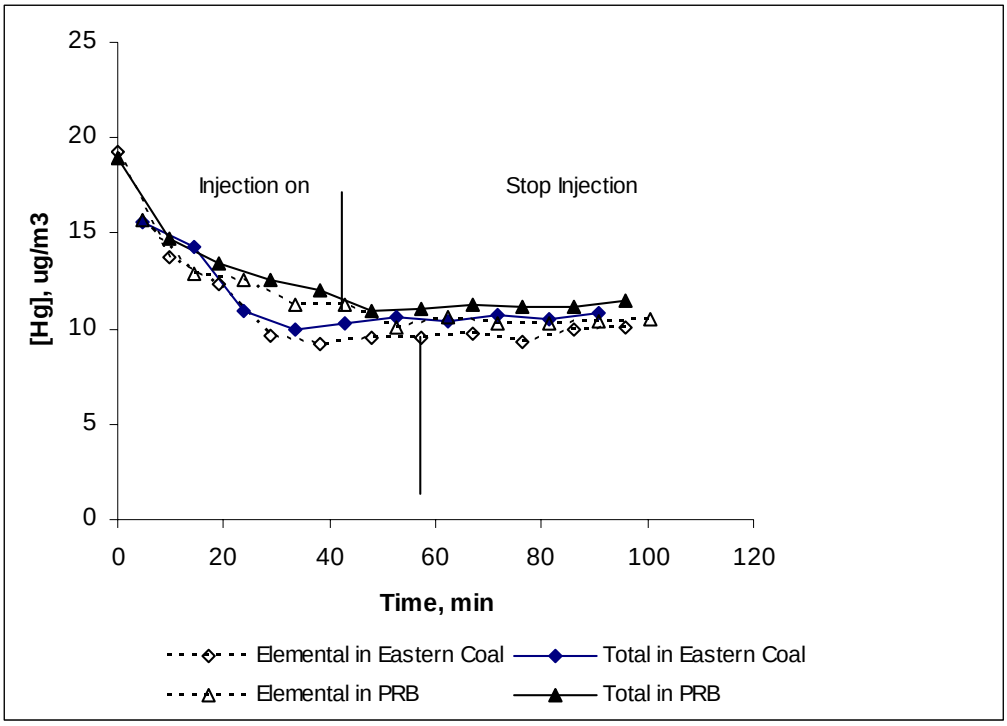

Figure 4.25. Entrained flow test results with Site 3 sample in Eastern coal and PRB flue gas at 140℃

The most likely reason for the different Hg removal performance with these AMD sorbents is the Fe_2O_3 content in the three samples. AMD Site 1 sample has only 3.7% of Fe_2O_3 while in Site 2 sample and 3 sample have 27.1% and 39%, respectively.

4.3.8 Entrained flow tests with Fe_2O_3 chemical in Eastern coal and PRB flue gas at 140°C

In this test, Fe_2O_3 powder (Fisher Scientific, Pittsburgh, PA) was injected at 140°C in eastern coal flue gas at the injection rate of 0.23 g/hr resulting in sorbent loading in the simulated flue gas of 0.31 g/m^3 and the ratio of sorbent/Hg of 17200. Fe injection rate is calculated as 0.217 g/m^3. The average particle size of Fe_2O_3 used in this test is 4.64μm. Performance of Fe_2O_3 is compared with the performance of Site A, 1, 2 and 3 samples in Figure 4.26. Compared with

Site A injection test, the final Hg removal efficiency with Fe_2O_3 was about 17% lower (it was about 68%). On the other hand, compared with Site 1 and 2 samples, Fe_2O_3 shows higher Hg removal efficiency even at lower sorbent load in flue gas (0.31g/m^3 vs.0.33g/m^3, 0.34 g/m^3).

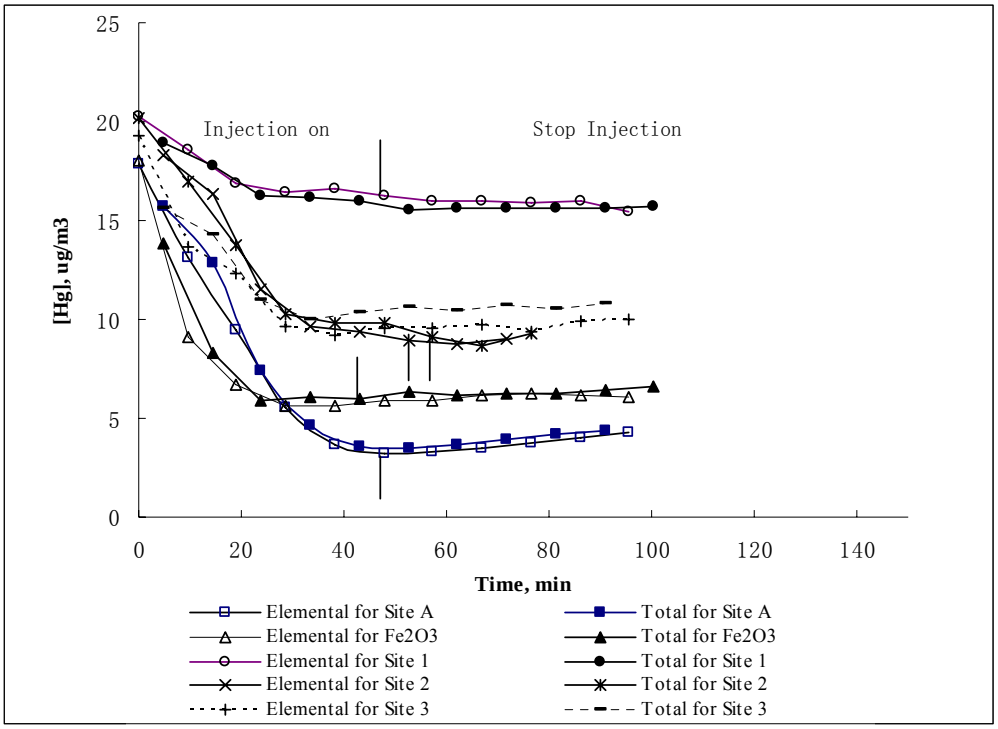

Figure 4.26. Fe_2O_3 chemical entrained flow test results compared with Site A, 1, 2 and 3 samples in Eastern coal flue gas at 140℃

Table 4.8 summaries the injection test results with different sorbents with respect to Fe% in the sorbent, sorbent injection rate and Fe injection rate of each sample. Fe injection rate is calculated by multiplying Fe% with sorbent injection rate. This table shows that most iron content was injected in the test with Site A sample and the highest Hg removal efficiency was achieved with Site A sample. In addition, Site 1 sample shows lowest Hg removal efficiency with lowest Fe injection rate.

Table 4.8. Fe%, Sorbent injection rate, Fe injection rate and [Hg] removal efficiency results in the entrained flow tests with eastern coal flue gas

Sample	Fe%	Injection rate, g/m^3	Fe injection rate, g/m^3	Hg removal efficiency,%
Site A at low injection rate	42.7	0.39	0.167	80
Site A at high injection rate	42.7	0.76	0.324	95
Site 1	2.59	0.34	0.009	26
Site 2	19.01	0.33	0.063	49
Site 3	27.30	0.30	0.082	53
Fe_2O_3	70	0.31	0.217	68

Figure 4.27 shows Hg removal as Fe injection rate for the tests with these five sorbents. It is clear that there is also a positive correlation between Hg removal and Fe injection rate as shown in this figure. Higher Fe injection rate resulted in higher level of mercury removal. Therefore, this finding suggests AMD sludge with high Fe content is preferred as sorbent for Hg removal.

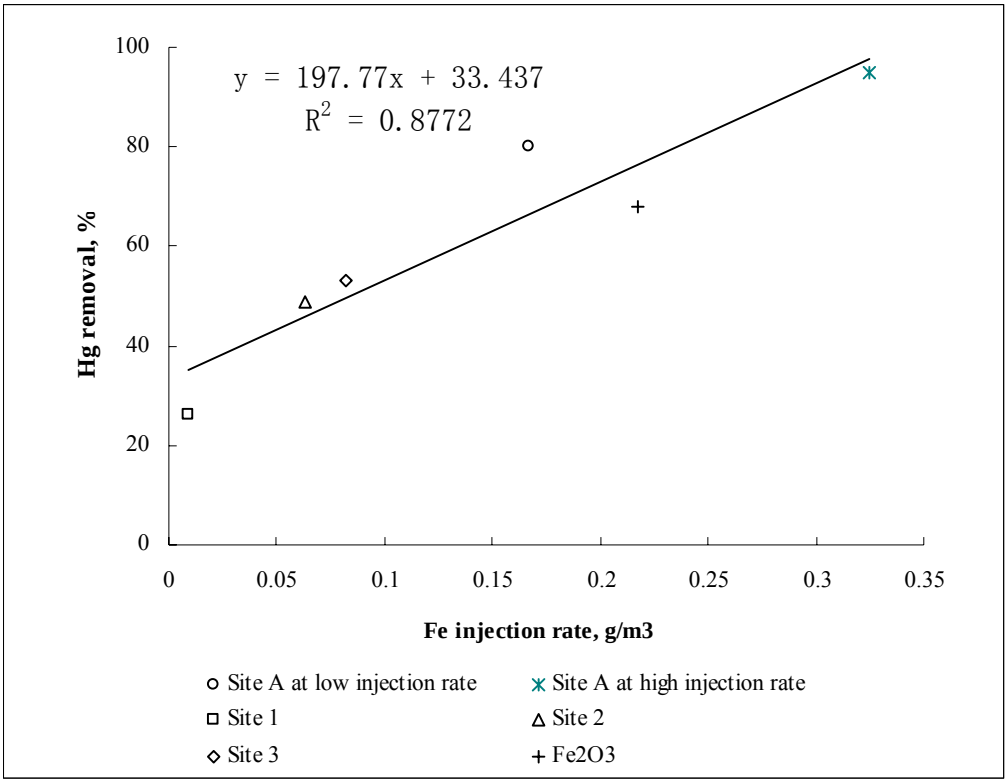

Figure 4.27. Fe injection rate and Hg removal results with Site A, 1, 2, 3 and Fe_2O_3 injection

4.4 FOAM INDEX TEST RESULTS

The test results summaried in Table 4.9 show that the Foam Index of Portland cement and AMD material used in this study is very close (between 24~ 31). On the other hand, the foam index of CE1 fly ash, which has 3.1% LOI, is more than 3 times higher (i.e.107)

Table 4.9 Foam Index test results of Portland cement and AMD samples

Sample	Foam index
Portland Cement	31
Site A	30
Site B	28
Site 1	27
Site 2	26
Site 3	24
CE1	107

These results suggest that AMD sorbents will not have any adverse impact on the amount of AEA needed for concrete production. Therefore, when AMD sorbents are injected in the coal-fired power plants for Hg removal application, this material will not cause negative effect on the quality of fly ash for cement applications.

5.0 SUMMARY AND CONCLUSIONS

Abandoned mine drainage (AMD) solids from different sites showed considerable capability of absorbing and oxidizing Hg^0 in fixed-bed tests. For Site A sample, NO and SO_2 individually could not cause any mercury uptake and oxidation without O_2. Addition of NO_2 to flue gas could help capture mercury even without the existence of O_2. HCl shows the greatest impact on Hg capture in the fixed-bed test and the role of O_2 was proved to be not as important for this reaction. When SO_2 and NO_2 participate in the reaction with HCl, evident decrease of mercury capture and oxidation was observed. The combination of SO_2 and NO in reaction with HCl prohibited mercury uptake.

In the entrained flow tests with Eastern coal and PRB coal flue gas, Site A solids displayed the highest Hg removal efficiency (about 80% Hg removal with 0.39 g/m^3 injection rate). The mercury removal efficiency achieved by Site 1, Site 2 and Site 3 solids under identical conditions was 26%, 45~55% and 50%, respectively. Therefore, this material shows potential for use in mercury emission control technology. There is evidence showing that high mercury removal efficiency is positively related to the Fe injection rate. Thus, AMD sludge with high Fe content is preferred as mercury removal sorbent.

Each AMD solids samples used in this study shows lower foam index number compared with standard commercial cement. Therefore, the use of AMD solids as mercury removal sorbents will not have adverse effect on the fly ash for concrete making application.

6.0 FUTURE WORK

In this study, AMD solids shows potential value as a novel sorbent for Hg removal in mercury emission control technology. This conclusion is drawn based on the lab-scale experiments. In order to evaluate the realistic performance of AMD solids for Hg removal, it is highly recommended to conduct pilot scale tests using this novel material in coal fired power plants. In addition, SO_3 in flue gas was found to significantly reduce Hg removal efficiency when ACI technology was used.[54, 55] It will be important to investigate the impact of SO_3 on Hg uptake and oxidation by this AMD sludge material in both fixed bed and entrained flow systems.

BIBLIOGRAPHY

1. Pavlish, J.H., Sondreal, E.A., Mann, M.D., Olson, E.S., Galbreath, K.C., Laudal, D.L., Benson, S.A. Status review of mercury control options for coal-fired power plants. Fuel Process Technology 2003, (82), 89-165.

2. Ackman, T. E. Sludge Disposal from Acid Mine Drainage Treatment; USBM RI 8672, 1982, 25 pp.

3. Chen, X. Impact of fly ash, its composition and flue gas components on mercury speciation in simulated flue gas. University of Pittsburgh, Pittsburgh, 2007.

4. Norton, G. A. Heterogeneous oxidation of mercury in simulated post combustion conditions. Fuel 2003, 82, 107-116.

5. Matt, L. Reducing Mercury Pollution from Power Plants, Issues in Science and Technology [http://www.allbusiness.com/technology/3583400-1.html], (Accessed at July 1, 2002)

6. Lu, D.Y., Granatstein, D.L., Rose, D.J. Study of Mercury Speciation from Simulated Coal Gasification. J. Ind. Eng. Chem. Res. 2004, 43, 5400-5404.

7. Presto, A., Granite, E.J. Survey of Catalysts for Oxidation of Mercury in Flue Gas. Environ. Sci. Technol. 2006, 40, 5601-5609.

8. EPA. Mercury Study Report to Congress Volume I: Executive Summary. Dec, 1997.

9. EPA. Information Collection Request for Electric Utility Steam Generating Unit Mercury Emissions Information Collection Effort. Apr, 1999.

10. Kilgroe, J.D. Mercury emission control study: preliminary results. In The Air Quality II: Mercury, Trace Elements, and Particulate Matter Conference, McLean, VA, 2000.

11. Chu, P., Goodman, N., Behrens, G., Roberson, R. In Total and speciated mercury emissions from U.S. coalfired power plants,, Proceedings of the Air Quality II: Mercury, Trace Elements, and Particulate Matter Conference, McLean, VA, 2000.

12. Senior, L.C., Sarofim, A.F., Zeng, F. In Predicting the speciation of mercury emissions from coal-fired power plants, Proceedings of the Air Quality II: Mercury, Trace Elements, and Particulate Matter Conference, McLean, VA, 2000.

13. EPRI. An Assessment of Mercury Emissions from U.S. Coal-Fired Power Plants, Palo Alto, CA, 2000.

14. Amrhein, G.T., Holmes, M.J., Bailey, R.T., Kudlac, G.A., Downs, W., Madden, D.A. Advanced Emissions Control Development Program, Phase III—Approved Final Report; July, 1999.

15. Laudal, D. L. Pilot-Scale Evaluation of the Impact of Selective Catalytic Reduction for NO, on Mercury Speciation, Report for EPRI, U.S. Department of Energy National Energy Technology Laboratory; 2000.

16. EPA. Controlling Power Plant Emissions: Mercury-Specific. http://www.epa.gov/mercury/control_emissions/tech_merc_specific.htm. Date accessed: Dec 10, 2008.

17. Bustard, J., Durham, M., Starns, D., Lindsey, C., Martin,C., Schlager, R., Baldrey, B. Full-scale evaluation of sorbent injection for mercury control on coal-fired power plants. Fuel Processing Technology 2004, 85, 549– 562.

18. Pavlish, J. H. Field Testing of Activated Carbon Injection Options for Mercury Control atTXU's Big Brown Station. In DOE NETL Mercury Control Technology Conference Pittsburgh, PA, 2007.

19. Nelson, S.J., Landreth, R. Accumulated Power-Plant Mercury-Removal Experience with Brominated PAC Injection. In the Combined Power Plant Air Pollutant Control Mega Symposium, Washington, DC, 2004.

20. Millera, S.J., Dunham, G.E., Olson, E.S., Brown,T.D. Impact of flue gas constituents on carbon sorbents, In Proceedings of the Air Quality II: Mercury, Trace Elements, and Particulate Matter Conference, 2000.

21. Boxley, C.H., Akash,A., Siegel,V. Treatment of high carbon fly ash for concrete applications. American Chemical Society 2008, 53 (1), 31-32.

22. Wu, S., Uddin, A. Characteristics of the removal of mercury vapor in coal derived fuel gas over iron oxide sorbents. Fuel 2006, 85, 213-217.

23. Wu, S., Ozaki, M. Development of iron-based sorbents for Hg^0 removal from coal derived fuel gas: Effect of hydrogen chloride. Fuel 2008, 87, 467-473.

24. Lee, J. Y. Development of Cost-EffectiveNoncarbon Sorbents for Hg^0 Removal from Coal-Fired Power Plants. Environ. Sci. Technol 2006, 40, 2714-2719.

25. Dunham, G.E., Dewall, R.A., Senior, C.L. Fixed-bed studies of the interactions between mercury and coal combustion fly ash. Fuel Process. Technol 2003, 82, 197-213.

26. Ghorishi, S.B., Lee, C.W., Jozewicz, W.S., Kilgroe, J.D. Effects of fly ash transition metal content and flue gas HCl/SO_2 ratio on mercury speciation in waste combustion. Environ. Eng. Sci. 2005, 22, 221-227.

27. Galbreath, K., Zygarlicke, C., Tibbetts, J. Effects of NOx, α-Fe_2O3, γ-Fe_2O_3, and HCl on mercury transformations in a 7-kW coal combustion system. Fuel Process.Technol 2004, 86, 429-448.

28. Wu, S., Ozaki, M. Development of iron oxide sorbents for Hg^0 removal from coal derived fuel gas: Sulfidation characterisitics of iron oxide sorbents and activity for COS formation during Hg^0 removal. Fuel 2007, 86, 2857-2863.

29. Qiu, J., Kong, F., Ai., Z, liu, H., Xing, W., Song, X. Experimental study of element mercury oxidation by α-Fe_2O_3 and γ-Fe_2O_3 nanoparticles. Am. Chem. Soc 2008, 53 (1), 75-76.

30. Watzlaf, G.R., Schroeder, K.T. The Passive Treatment of Coal Mine Drainage; Pittsburgh, 2004.

31. Yeh, S., Jenkins, C.R. Disposal of sludge from acid mine water neutralization. J. Water Pollut. Control Fed 1971, 43 (4), 679-683.

32. Roger, C., Viadero, J. Wei, X., Buzby, K.M. Characterization and Dewatering Evaluation of Acid Mine Drainage Sludge from Ammonia Neutralization. Environmental Engineering Science, 2006, 23 (4), 734-743.

33. Kirby, C.S. Decker, S.M. Comparison of color, chemical and mineralogical compositions of mine drainage sediments to pigment. Environ. Geol 1999, 37 (3), 243-247.

34. Coal Research Bureau. Dewatering of Mine Drainage Sludge; EPA: Washington, DC, 1971.

35. Hedin, R.S. Recovery of iron oxides from polluted coal mine drainage April 15,1997.

36. Weia, X., Viadero, R.C., Bhojappaa, B. Phosphorus removal by acid mine drainage sludge from secondary effluents of municipal wastewater treatment plants. Water Resource 2008, 42 (13), 3275-3284.

37. Fish, C.L., Hedin, R. S., Partezana, J.M. Chemical characterization of iron oxide precipitates from wetlands constructed to treat polluted mine drainage. In Natl Meet Am Soc Surf Mining and Recl, Knoxville, 1996; pp 541-549.

38. Miller, S.J., Dunham, D.E., Olson, E.S., Brown, T.D. Flue gas effects on a carbon-based sorbent. Fuel Process. Technology 2000, 65-66, 343-364.

39. Bhardwaj, R. Impact of temperature and flue gas components on mercury speciation and uptake by activated carbon sorbents. University of Pittsburgh, Pittsburgh, 2007.

40. Kűlaots, I., Hsu, A., Hurt, R.H., Suuberg, E.M. Adsorption of surfactants on unburned carbon in fly ash and development of a standardized foam index test. Cement and Concrete Research 2003, 33, 2091-2099.

41. Stencel, J.M., Songa, H., Cangialosi, F. Automated foam index test: Quantifying air entraining agent addition and interactions with fly ash–cement admixtures. Cement and Concrete Research. 2009.

42. Laudal, D. L., Brown, T. D., Nott, B. R. Effects of flue gas constituents on mercury speciation. Fuel Processing Technology 2000, (65-66), 157-165.

43. Cao, Y., Chen, B., Wu, J., Cui, H., Smith, J., Chen, C. Study of Mercury Oxidiation by Selective Catalytic Reduction Catalyst in a Pilot-Scale Slipstream Reactor at a Utility Boiler Burning Bituminous Coal. Energy & Fuels 2007, 21, 145-156.

44. Eswaran, S., Stenger, H.G. Understanding mercury conversion in selective catalytic reduction (SCR) catalysts. Energy & Fuels 2005, 19, 2328-2334.

45. Sliger, R.N., Kramlich, J.C., Marinov, N.M. In Development of an elementary homogeneous mercury oxidzation mechanism, Proceedings of the 93rd Air and Waste Management Association Annual Meeting, Salt Lake City, UT, 2000.

46. Wang, J., Cobb Jr, J.T., Elder, W.W. Study of mercury oxidation in the post-combustion zones of coal-fired boilers. American Chemical Society, Division of Fuel Chemistry Preparation 2001, 46.

47. Galbreath, K. C., Zygarlicke, C. J. Mercury Speciation in Coal Combustion and Gasification Flue Gases. Environ. Sci. Technology, 1996, 30 (8), 2421-2426.

48. Olson, E. S., Dunham, G. E., Sharma, R. K., Miller, S. J. Mechanisms of mercury capture and breakthrough on activated carbon sorbents. In American Chemical Society National Meeting,, Washington DC, 2000; pp 886-889.

49. Rubel, A., Andrews, A., Gonzalez.R., Groppo.J., Robl, T. Adsorption of Hg and NOx on coal by-products, Fuel, 2005, 84 (7-8), 911-916.

50. Carey, T.R., Hargrove, O. W. Richardson, C.F., Chang, R. Factors Affecting Mercury Control in Utility Flue Gas Using Activated Carbon Journal Of The Air & Waste Management Association 1998, 48, 1166-1174

51. Wu, J., Cao, Y., Pan, W., Shen, M., Ren, J., Du, Y., Wu, J., Cao, Y., Pan, W., Shen, M., Ren, J., Du, Y., He, P., Wang, D., Xu, j., Wu, A., Li, S., Lu, L., Pan, W. Evaluation of mercury sorbents in a lab-scale multiphase flowreactor, a pilot-scale slipstream reactor and full-scale power plant. Chemical Engineering Science 2008, 63, 782-790.

52. Ghorishi, S.B., Keeney, R.M. Development of a Cl-Impregnated Activated Carbon for Entrained-Flow Capture of Elemental Mercury. Environ. Sci. Technol. 2002, 36, 4454-4459.

53. Granite, E.J., Pennline, H.W., Hargis, R.A. Novel Sorbents for Mercury Removal from Flue Gas. Ind. Eng. Chem. Res. 2000, 39, 1020-1029.

54. Campbell, T. Influence of SO_3 on Mercury Removal with Activated Carbon: Full-Scale Results; ADA-ES, Inc: 2008.

55. Miller, S., Richardson, C. Implications of SO_3 removal on mercury capture. In Proceedings of the 2006 Environmental Controls Conference, URS Corporation, 2006.